NTNU
Norwegian University of
Science and Technology

Condition Assessment of Medium Voltage Cable Accessories

PD Measurements at Variable Frequencies

Gunnar Stokke Einan

Master of Energy and Environmental Engineering
Submission date: July 2016
Supervisor: Frank Mauseth, ELKRAFT
Co-supervisor: Sverre Hvidsten, SINTEF Energi AS

Norwegian University of Science and Technology
Department of Electric Power Engineering

Title:	Condition Assessment of Medium Voltage Cable Accessories
Student:	Gunnar Einan

Problem description:

A significant part of the Norwegian medium voltage cable distribution net is older than the expected lifetime of 30 years. Cable joints have a shorter expected lifetime than the cable. In case of heat-shrink joints installed in the 80's, many service failures have occurred due to over-heating of the metallic connector. In general, the condition of the insulation of the joints can be assessed by partial discharge measurements or dielectric spectroscopy. For joints and terminations, field grading materials (FGM) are often used to achieve the wanted field distribution to avoid local field enhancement and partial discharges. The dielectric properties of the FGM will also be influenced by the frequency of the applied voltage, but also humidity and temperature will influence the resulting field distribution.

The project work will be mainly experimental. The student will do preparing work for investigation of the field and frequency dependency of the field grading material. For the laboratory tests, the student will use an already existing set-up for PD testing in the frequency range of 0.01 to 200 Hz. Test objects with an embedded hollow microsphere will be made to test if the the hollow microspheres are suited for further testing in FGM. A simulation model will be made to check the field strength inside the microsphere. The data from the measurements will be analysed with different methods.

Supervisor:	Frank Mauseth, NTNU ELKRAFT
Co-supervisor:	Sverre Hvidsten, SINTEF ENERGI AS

Preface

This masters thesis is written in the spring semester 2016 as a part of the study in Energy and Environmental Engineering. The work is given from Department of Electric Power Engineering in collaboration with SINTEF Energi AS.

First of all I would like to thank my responsible supervisor, Associate Professor Frank Mauseth, for great help throughout the whole year. Both his scientific knowledge and his practical knowledge have been very valuable, especially during long days in the lab.

I would also like to thank my co-supervisor, Senior Research Scientist Sverre Hvidsten, for being helpful in his busy schedule. His advises have been motivating during times of adversity.

Lastly I would like to thank Hans Helmer Sæthernes for good help in the preparation of the test objects and Espen Eberg for help during this work and for the Matlab-scripts.

Abstract

Diagnostic PD testing of medium voltage cables can be performed at very low frequencies (VLF, 0.1 Hz), to reduce capacitive currents. At 0.1 Hz the field distribution in the field grading materials is likely different from the one at power frequency, possibly leading to wrong conclusions from the tests. The frequency dependency of such materials, can be investigated using previously tested PD sources, where different PD parameters have been characterised as function of frequency. In this work, it was tested if hollow glass microspheres were suited as such a PD source.

The spheres were molded into a silicone cup and tested under a uniform field. Before each test, the test object was electrical conditioned for 16.5 hours either at 6 kV at 50 Hz or at ground potential to have equal initial conditions. The PD inception and extinction voltage were tested as indicators of the field strength at the site of the spheres. These parameters were, among others, found for selected frequencies in the range from 0.1 to 50 Hz. The data was recorded during the tests and later analysed with PRPD-, Weibull- and pulse sequence analysis. A finite element simulation was performed to find the relation between the applied voltage and the field strength inside the glass sphere.

The tests showed a great dependency on the initial condition, with a higher PD inception voltage after a period of grounding. This showed the importance of an equal initial condition and a standardized conditioning period before each test. The inception voltage varied a bit, but the extinction voltage was more consistent and found to be a good parameter for determining the field strength inside the spheres. The cavity discharges gave characteristic and easily recognizable patterns in the PRPD-analysis, the shape parameters in the Weibull distributions were consistent with the literature and the pulse sequence analysis confirmed the earlier findings and could also reveal periods without discharges. The start electron availability decreased during a long period of many test series, causing the discharge characteristics to change, but still being consistent with cavity discharges. A relation between the applied voltage and the field strength inside the spheres was found through the FEM simulations and the decrease in the repetition rate with decreasing voltage.

Based on these findings, the spheres can be suited for testing, if the start electron availability reaches a steady state. The PD extinction voltage is a reliable parameter suited for determining the field strength at the site of the sphere.

Sammendrag

Diagnostisk testing av kabler kan utføres med PD testing ved veldig lave frekvenser (VLF, 0,1 Hz), dette for å redusere den kapasative strømmen. Feltfordelingen vil være forskjelling i de feltstyrende materialene ved testfrekvensen og nettfrekvensen, dette kan føre til at feil konklusjoner trekkes fra testene. Frekvensavhengigheten til slike materialer kan sjekkes med en tidligere testet PD-kilde, hvor forskjellige PD-parametre har blitt karakterisert som funksjon av frekvens. I dette arbeidet ble det testet om hule mikroglasskuler er passende PD-kilder.

Kulene ble støpt inn i en silikonkopp som be testet under et uniformt felt. Før hver test ble testobjektet elektrisk kondisjonert i 16,5 timer, enten på 6 kV ved 50 Hz eller ved jordpotensiale for å ha like startbetingelser. Tenn- og slukkespenning ble testet som feltstyrkeindikatore ved kulens plassering. Disse parameterene ble, sammen med fler, funnet for valgte frekvenser i området fra 0,1 til 50 Hz. Dataene fra testene ble lagret og senere analysert med PRPD-, Weibull- og pulssekvensanalyse. En FEM-simulering ble gjort for å finne forholdet mellom den påtrykte spenningen og feltstyrken inne i kula.

Testene viste avhengighet av den initielle tilstanden, hvilket ga en høyere tennspenning etter en jordingsperiode. Dette viste viktigheten av å ha like startbetingelser og en standardisert kondisjoneringsperiode før hver test. Tennspenning ble funnet til å variere, men slukkespenningen var mer konsistent og ble funnet til å være en god parameter for bestemme feltstyrken ved kulenes plassering. Hulromsutladningene ga karakteristiske og lett gjenkjennelige plott i PRPD-analysen, formparametre i Weibull-analysen som var konsistente med litteraturen og pulssekvensanalysen bekreftet de tidligere funnene og kunne også avsløre flere perioder uten utladninger. Tilgjengeligheten av startelektron ble dårligere i løpet av et langt tidsrom med mange testserier. Dette førte til at utladningskarakteristikken ble endret, men den var fremdeles konsistent med hulromsutladninger. Det ble funnet et forhold mellom den påtrykte spenningen og feltstyrken inne i kula, på grunnlag av FEM simuleringene og reduksjonen i repetisjonsraten ved avtagende spenning.

Basert på disse funnene kan kulene være egnet til videre testing, under den forutsetning om at tilgjengeligheten av startelektron når en stabil tilstand. Slukkespenningen er en passende parameter for å bestemme feltstyrken ved kulens plassering.

Contents

1 Introduction

For cable joints and terminations, field grading materials are often used to achieve the wanted field distribution and avoiding a large local field enhancement, where the outer semiconductor is terminated. The dielectric properties of the field grading material are frequency dependent, which will change the field distribution with different frequencies. The field strength in a cavity within a joint or termination will therefore be dependent on both the frequency and the location of the cavity. If the field strength inside the cavity is above the critical withstand strength of the gas, partial discharges (PD) can occur inside the cavity. PDs can lead to an irreversible degradation of the insulation material and eventually total breakdown of the whole insulation material [1].

Cable diagnostics are often performed with partial discharge measurements. To reduce the capacitive currents and thereby reducing the size and cost of the measuring equipment, the test can be performed at very low frequencies, such as 0.1 Hz [2]. A cavity within a cable joint or termination will not be exposed the same field strength at the test frequency, as it would at power frequency at the same voltage. Thus, can detection of partial discharges in the tests be dependent of the location of the cavity and not consistent with the situation at 50 Hz.

The scope for this task is to find if hollow glass microspheres are suited for testing the location and frequency dependency for cavities within joints and terminations. To investigate the frequency dependence of the field grading the materials, a hollow microsphere can be placed at different locations in a cable termination to determine the field strength distribution. The field strength is determined by the occurrence of PD in the microspheres. The PD inception voltage (PDIV) and the PD extinction voltage (PDEV) are two easy measurable field strength indicators, which need to be characterised.

The microspheres will need to give recognizable PD patterns, show consistency in the results and no sign of ageing. To find the PDIV, a hollow microsphere was

molded into a silicone cup which was placed under an uniform electric field, and the voltage was risen in stages until repetitive PDs of a certain size was detected. PDEV was found by decreasing the voltage until repetitive PDs of a certain size ceased. The data collected from these tests were further analysed with pulse sequence analysis and Weibull analysis. In addition to these tests, a finite element simulation of the silicone cup with a microsphere was performed, to check the relation between the applied voltage and the field strength inside the microsphere.

2 | Theory

2.1 Partial discharges

Partial discharges are defined as localized electrical discharges that only partly bridges the insulation material [3]. Two initial conditions need to be fulfilled to have a PD. An electric field which is high enough to initiate an electron avalanche is required, the electron avalanche typically will start on sharp edges which gives a local field enhancement. The dielectric strength of the insulation need to be low enough for the local insulation to breakdown. An air filled cavity in cable insulation will have lower dielectric strength than the rest of the insulation. Therefore, it is most likely to have a breakdown in the cavity.

There is also a statistical requirement that need to be fulfilled. An initial free electron must be present. The free electron will be accelerated by the electric field and may cause an ionizing collision, which may lead to a breakdown of the cavity. If the electron is not present when the electric field is above the critical value for starting a discharge, the discharge can not be initiated. The discharge will first take place when a free electron appear, the average waiting time between the two events is called the statistical time lag. The time lag decreases with increasing voltage due to higher rate of electron surface emission [4]. The detrapping rate of trapped electrons is the dominating part of the surface emission rate. It is exponentially dependent on the field strength inside the cavity [5], which reduces the time lag for increasing voltage. In virgin cavities, *i.e.* cavities with no previous PD activity, the waiting time for the first electron is controlled by the ionizing effect of the cosmic and radioactive radiation. The waiting time is dependent on the void diameter. For spherical voids with a diameter of 500 µm the average waiting time is about 3 hours [6].

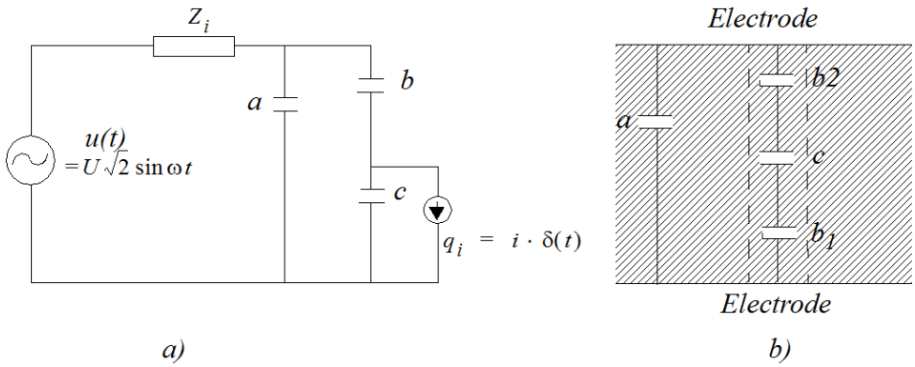

Figure 2.1: *abc*-equivalent circuit [7, p.215].

2.1.1 *abc*-model

Gas filled cavities in solid insulation are a common reason for PD-activity in cable insulation. The *abc*-model is a model where the different parts of the insulation is represented as capacitances in an electric circuit. c is the capacitance of the cavity, b_1 and b_2 is the capacitance of the insulation above and below the cavity, the stray capacitance, and a is the capacitance of the rest of the insulation, which has an area equal the total area except for the area of the cavity. For plane electrodes with a cavity, which only have surfaces parallel and normal to the electrodes, the capacitances are given by:

$$C = \frac{\varepsilon_0 \varepsilon_r A}{d}, \tag{2.1}$$

where C is the capacitance, ε_0 is the absolute permittivity, ε_r is the relative permittivity, A is the area of the surface perpendicular to the E-field and d is the length of the capacitance in the direction of the E-field. In this work the cavity is spherical shaped. Thus, the above capacitances are not completely correct, but the principle holds for the following explanations.

In general $a >> b$ is assumed because the area of the whole insulation is usually big compared to the area of the cavity. Normally $b < c$ because the height of the cavity is usually smaller than the total height of b_1 and b_2, which is combined into b [7].

The voltage over the cavity is proportional to the applied voltage. By applying the relation from capacitive voltage dividers, the voltage over the cavity is given by:

$$U_c(t) = \frac{b}{b+c}\sqrt{2}U\sin(\omega t), \tag{2.2}$$

where U is the RMS-value of the applied voltage on the test object and $U_c(t)$ is the alternating voltage across the cavity.

The electric field strength inside the cavity can be found with a field enhancement factor of the surrounding field:

$$E_{cav} = \frac{3\varepsilon_{r,sur}}{1+2\varepsilon_{r,sur}}E_{sur}, \tag{2.3}$$

where E_{cav} is the field strength inside the cavity, $\varepsilon_{r,sur}$ is the relative permittivity of the surrounding material and E_{sur} is the field strength in the surrounding material.

2.1.2 PDIV and PDEV

The voltage, U_i, where the first repetitive PDs occurs is defined as PDIV. The *abc*-model does not take the statistic waiting time into account. Thus, a PD will occur once the voltage across the cavity reaches the breakdown voltage. Figure 2.2 shows the applied voltage on the cavity which is given by (2.2) and the voltage across the cavity at the time of inception. The voltage across the cavity will drop to the remnant voltage, U_{r0}, due to the discharge [7]. The difference between U_{s0} and U_{r0} is in this model constant, in practice it may vary a bit due to the stochastic nature of PDs. If the applied voltage is further increased, the voltage across the cavity will reach U_{s0} more often [8]. Therefore, the repetition rate of the discharges increases and they will start to appear earlier on the phase. The discharges in each half cycle will stop just before or at the peak of the applied voltage, as shown in Figure 2.2

The PDEV, U_e, is the applied voltage at which PD pulses of a certain charge magnitude disappear when the voltage is decreased from a level where PD occurs [8]. For an applied voltage just above PDEV, there will only be one PD per half cycle at the peak of the applied voltage [7].

The critical field strength for initiating PDs, $E_{critical}$, can be found if the pressure and diameter of an air filled void is known. To find this, the Paschen curve [7] or the following equation can be used.

$$E_{critical} = (\frac{E}{p})_{cr}p(1+\frac{B}{(pd)^n}), \tag{2.4}$$

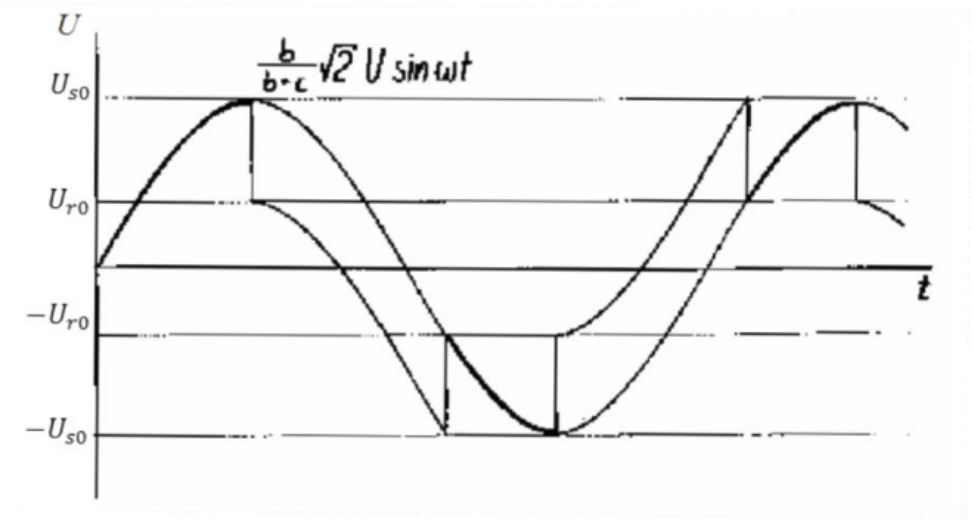

Figure 2.2: Applied voltage to the cavity and voltage across the cavity just after PDIV [7, p.219].

where $(\frac{E}{p})_{cr}$, B and n are associated to the ionization process of the gas, p is the pressure in the cavity and d is the diameter of the cavity. For air, $(\frac{E}{p})_{cr} = 24.2$ $\mathrm{VPa^{-1}m^{-1}}$, $n = 0.5$ and $B = 8.6$ $(\mathrm{Pa{*}m})^{1/2}$ [5].

2.1.3 Ageing

Having PDs in a void may cause an irreversible change in the properties of the insulation material at the PD site. This change is often referred to as ageing. To what extent and in which way the insulation material is affected, strongly depends on the material, the geometry of the void and the duration of the PD activity. An example of an ageing mechanism is erosion of the material, where the PD activity causes pits [9]. Another example is changes in gas pressure and gas composition [10]. Ageing often causes a change in the PD activity [11]. Thus, reproducible experiments may not be obtainable once an ageing mechanism has occurred.

Glass and ceramic materials are known for having the qualities necessary to withstand stress such as arcing [7]. The test objects in this work are made of such a material, and should not change the discharge properties due to ageing mechanisms.

2.1.4 PD measuring

To ensure reproducible results, it is recommended to choose among three test circuits in IEC 60270 [3]. Figure 2.3 shows a test circuit where the measuring impedance Z_m is connected in series with the coupling capacitor C_k, which is the most common test circuit. A noise canceling low pass filter is placed between HV transformer/ amplifier and the test object. The filter has two purposes, it reduces noise from the external grid and it prevents the PD signal from going through the HV transformer/amplifier. Placing Z_m in series with C_k compared to in series with the test object, is at the cost of lost sensitivity. But it is also a safer test circuit, because the current running through the test object might become extremely high and may damage Z_m, especially in case of a complete breakdown of the test object. To have decent measuring sensitivity the following condition should be satisfied: $C_k/a > 0.1$ [8].

The apparent charge q_a is a term introduced with the *abc*-model and is the charge transfer appearing at the terminals of the test object. The apparent charge transfer is not the same as the charge transfer in the cavity. The discharge in the cavity will cause a voltage drop across the cavity and draw a transient current Δi from C_k. To find the apparent charge, the transient current is integrated and gives the following relation:

$$q_a = \int \Delta i dt = \Delta U * a, \tag{2.5}$$

where ΔU is the voltage drop across the test object, and a is the capacitance of the test object [12].

Calibration

Calibration is necessary to perform accurate measurements on the test circuit. A known calibrating charge, q_0, is applied to the terminals of the test object, resulting in a reading R_0 on the PD measuring instrument. From these two values, a scaling factor is derived. The scaling factor applies to relation between the apparent charge, q_a, from a PD and the reading, R_i, from the same PD [8]:

$$q_a = \frac{R_i}{R_0} q_0 \tag{2.6}$$

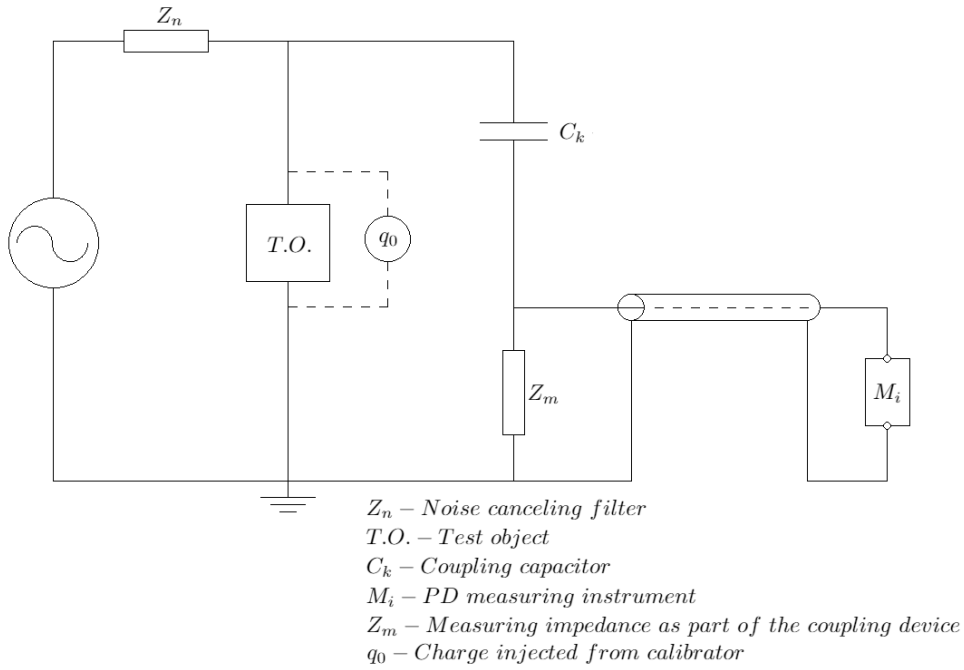

Figure 2.3: Basic PD test circuit recommended in IEC 60270 [8] with a charge calibrator connected through the dotted line.

2.1.5 PD charge

The apparent charge is calculated according to (2.5) when measured. The Niemeyer model presents a method of calculating the physical charge transfer for a PD. This is physical charge transfer inside the sphere, and does not account for losses from the discharge site to the measuring equipment:

$$\pm q = \pi \varepsilon_0 b^2 [1 + \varepsilon_r (K(\frac{a}{b}) - 1)] \Delta E, \tag{2.7}$$

where q is the charge transfer, b is the ellipsoidal radius perpendicular to E as described in Figure 2.4, ε_r is the relative permittivity of the surrounding material, $K(\frac{a}{b})$ is a function inverse of the polarization factor and ΔE is the change in E during a PD. $K(\frac{a}{b}) = 3$ for spherical cavities [6]. ΔE can be found with the Paschen curve [7] or (2.4).

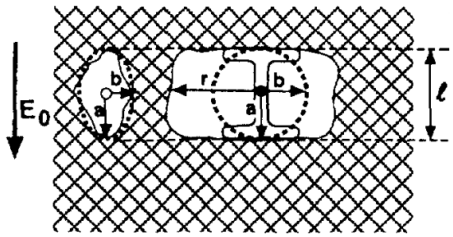

Figure 2.4: Examples of the approximate assignment of the equivalent ellipsoidal radius a and b needed to solve (2.7) [6].

2.1.6 Charges inside the cavities

Charges can accumulate on the inner surface of a cavity, how this happens and the consequences are explained in the following. The electric field inside a cavity, E_{cav}, has two components, as shown in Figure 2.5c. The first component is called the Laplacian field, which is a field proportional to the external applied field, E_0, with the factor f_c. The second component is called the Poisonnian field, E_s, and is caused by the charges accumulated on the surface.

Before a PD occurrs, the field inside the cavity is equal to the Laplacian field, as shown in Figure 2.5a. When a streamer inside the cavity develops, charges begin to accumulate on the surfaces close to the electrodes, as shown in Figure 2.5b. After the streamer extinction, charges have accumulated on the surface of the cavity. Thus, the Poisonnian field is present and causing a reduction in E_{cav}, as shown in Figure 2.5c [5].

Figure 2.6 explains how the charges inside the sphere are affected by the external field, E_{cav0} is in this figure the Laplacian field. Figure 2.6a shows a typical state after a PD event, with E_s opposing E_{cav}. The free charges are affected by the electric field and will tend to move along E_{cav}. In this case, the charges will be more concentrated at their site. Figure 2.6b shows a state where the direction of the applied field has changed and E_{cav} has the same direction as E_s. In this case the charges might drift through the gas or move along the cavity surface, causing recombination and a reduction of surface charge [5, 11].

2.2 PD analysis

The measured discharges are analysed both in real time during the measurements and afterwards. The following sections describe different methods used to analyse

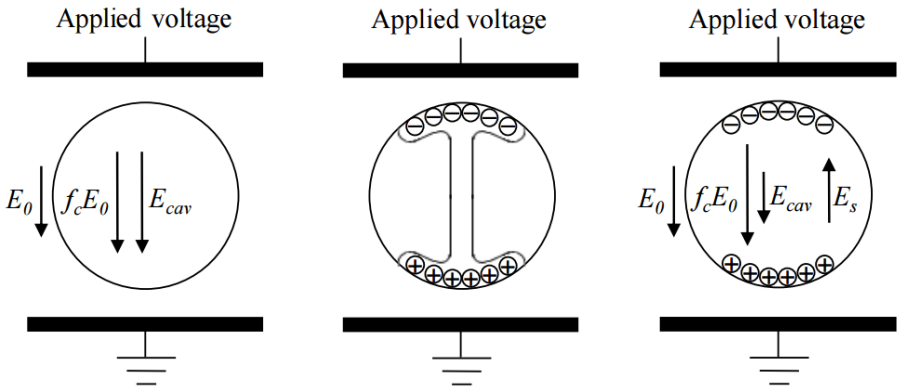

(a) Before PD **(b)** During PD **(c)** After PD

Figure 2.5: Schematic diagram of a PD event [5]. This figure shows the field inside the cavity before a discharge, the charge transfer during the discharge and the fields inside the cavity after a discharge.

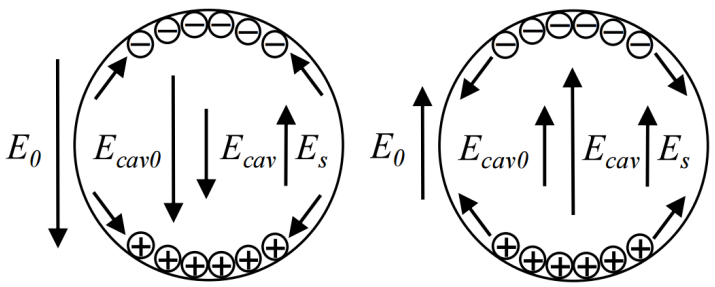

(a) E_{cav} has opposite direction to E_s. **(b)** E_{cav} has the same direction as E_s

Figure 2.6: Movement of PD free charges with different polarity of the applied field [5].

data from the measurements.

2.2.1 Phase resolved PD analysis

The discharges are first analysed in a phase resolved partial discharge (PRPD)-plots, produced by the Omicron software. This type of analysis is often called phase resolved partial discharge analysis (PRPDA). The PRPD-plots contain one period of the voltage, the charge amplitude of a discharge at the phase angle where the discharge happens and the intensity of the discharges is indicated with a color range. Figure 2.7 shows an example of a PRPD-plot.

Certain types of defects have characteristic shapes in a PRPD-plot [13]. Cavities can be characterized by discharges in the rising part of each half cycle with a quite constant charge amplitude, if the availability of start electrons are good. This can be explained by Figure 2.2, where the PDs occur in the rising part of the half cycle, when the voltage across the cavity reaches a certain limit. The number of discharges per period increases when the voltage is risen, and the discharges will appear earlier on the phase. The discharges may also appear on the decreasing part of the previous half cycle, if the voltage is risen well above PDIV. Even if these discharges may appear of the decreasing part of previous half cycle, this phenomena is referred to as PDs on the rising part of the half cycle in the rest of this thesis.

Figure 2.7 shows an example of PDs in a cavity, the size of the charges are quite constant and the discharges are occurring at the rising part of the half cycle. "Rabbit-ears" is also a common property for cavity discharges [14], and appear when the start electron availability is poor [5]. Other characteristic plots are found for air bubbles in oil and different pollutions [15, 16]. Another useful characteristic is the property that corona occurs at the peak of each half cycle [7, Fig. 4.14], [17, 18]. The measuring impedance is frequency dependent. Testing at different frequencies may therefore lead to a phase shift between the measured voltage and the recorded PDs. If a corona source is attached to the test object HV terminal the phase shift can be found.

2.2.2 Pulse sequence analysis

The pulse sequence analysis (PSA) is a method used to analyse a sequence of individual discharges. It can be used both to analyse the change in voltage level between following discharges and the time or phase difference between following discharges.

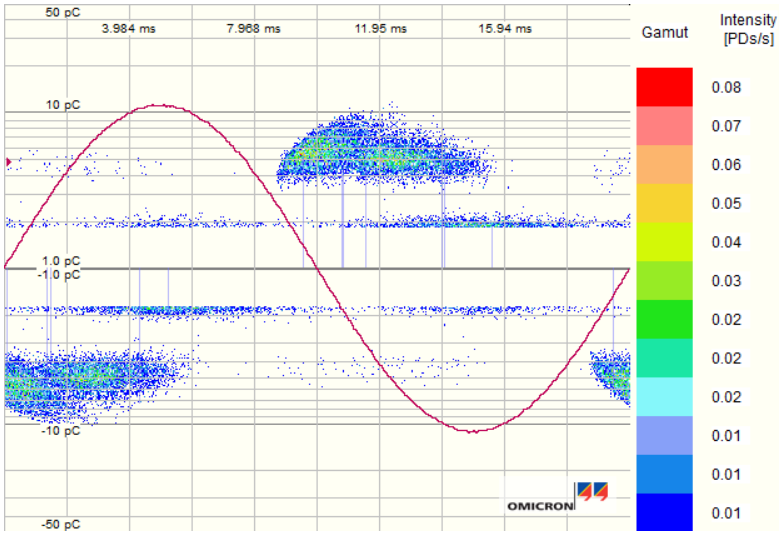

Figure 2.7: This is an example of a PRPDA-plot from the Omicron system. In this example the PD source is a void in the insulation, indicated by discharges on the rising part of the half cycle.

Figure 2.2 shows the voltage across a cavity just after PDIV is reached. The voltage drop at each half cycle is here constant, in practice it will vary a bit. In the instance of two or more discharges per half cycle, the voltage drops have quite constant size and is given by $U_{s0} - U_{r0}$. For two following discharges in the positive half cycle this change will be positive, and in the negative half cycle it will be negative. The voltage change between a discharge in the positive half cycle and a following discharge in the negative half cycle will be negative, and in the opposite case the change will be positive. The time difference between two following discharges will depend on the steepness of applied voltage. The largest time difference for discharges of the same polarity, will be between the two last discharges. The shortest time difference will be for the discharges closest to the zero passage.

In PSA the difference between following discharges is compared. Figure 2.8 shows a voltage curve with PD events, the figure describes how the voltage differences are found and plotted. Plotting a longer sequence of PDs might reveal some trends, some characteristic plots are related with certain discharge mechanisms. Figure 2.9 shows PSA-plots for two different discharge sources.

In addition to the PSA plots, it can be interesting to look at the cumulative distribution of both the time differences and the voltage differences. These plots give a better picture of the distribution of the differences, compared to the PSA plots where the intensity might be difficult to evaluate.

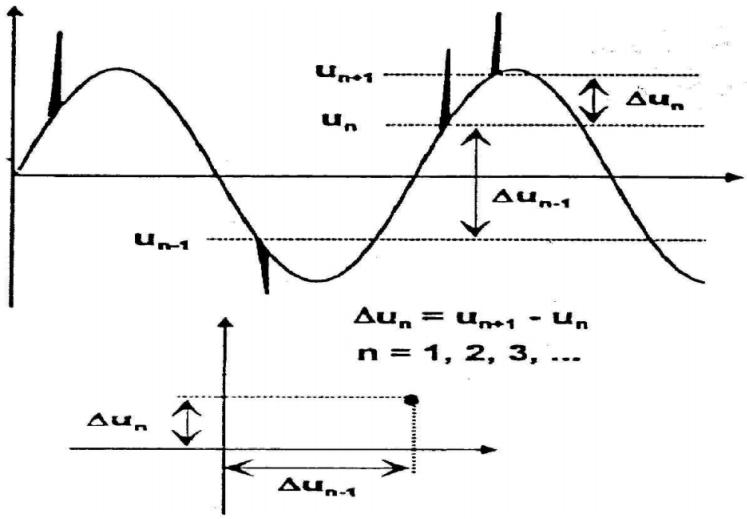

Figure 2.8: Explanation for plotting voltage difference PSA [19]. The upper figure shows a voltage signal with PD events. $\Delta V_n = V_{n+1} - V_n$ is the voltage difference between the next PD event, $n+1$, and the n^{th} PD event. $\Delta V_{n-1} = V_n - V_{n-1}$ is the voltage difference between the n^{th} PD event, and the previous PD event, $n-1$. The lower figure shows how a point is plotted in a PSA-plot for the given PD events.

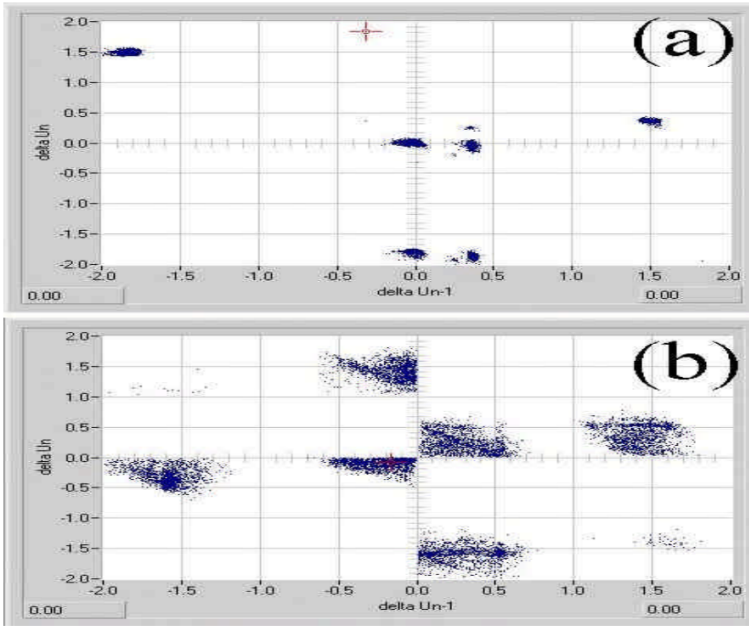

Figure 2.9: Examples of characteristic PSA-plots [19]. The figure shows discharges in cable sealing ends (a) for PD in a cavity (b) for surface discharges.

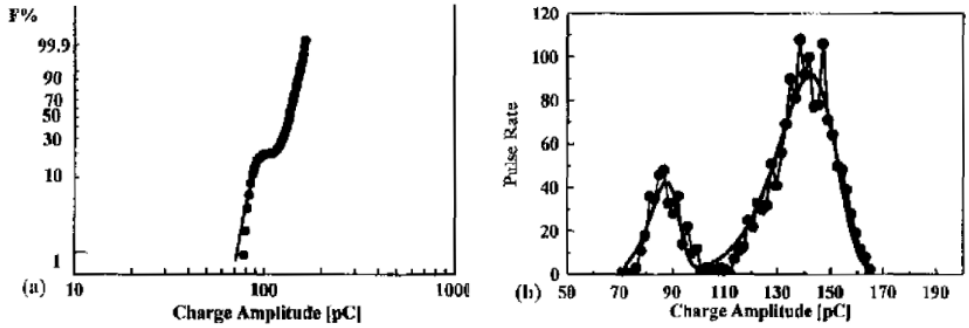

Figure 2.10: Examples of cumulative (a) and density(b) distributions for discharges caused by two different corona sources [20].

2.2.3 Weibull analysis

It is shown that the Weibull distribution have a good fit to the PD height distribution, and the shape parameter, β, is related with the discharge mechanism. This method has also shown good results in separating two simultaneously occurring PD mechanisms. In the case of two PD sources the 5-parameter Weibull distribution is used:

$$F(q) = pF_1(q) + (1-p)F_2(q), \tag{2.8}$$

where q is the charge magnitude, p is the set of the first sub-population, F_1, and F_1 and F_2 are sub-populations given by:

$$F(q) = 1 - exp[-(\frac{q}{\alpha})^{\beta}], \tag{2.9}$$

where α is the scale parameter and β is the shape parameter [20, 21].

When the 2 parameter cumulative distribution is plotted in a logarithmic scale the curve is linear. For a 5-parameter distribution the curve has two linear segments, which is shown in Figure 2.10, this property makes graphical analysis possible. Analysis is also possible through use of analytical software, in this work Matlab is used. The data is fitted to a 5-parameter cumulative distribution using maximum likelihood estimation [22].

3 | Method

3.1 The test objects

The test objects are molded silicone cups, with a hollow alumina-silica microsphere centered in the bottom of each cup. Different molding processes and thicknesses of the test objects have been tested. To have a small PDIV is preferable, this reduces the chance of activating other discharge sources before a PD in the cavity occurs. By reducing the thickness of the test objects the PDIV is reduced. The smallest manageable thickness is the one chosen.

The microspheres may have some damages, an elliptical shape or different diameters. Therefore, they need to be inspected in a microscope before the molding process. The ones without any visual imperfections and a diameter of approximately 500 µm were selected.

3.1.1 Making the test objects

The procedure of making the test objects is described in the following three steps:

1. A circular plate with a thickness of 0.25 mm is made in a mold with an inner diameter of 10 cm.
2. The plate from the previous step is placed in the bottom of the same mold, further a hollow microsphere is placed on the center of the plate. Liquid silicone is applied and molded to a 0.75 mm thick plate. For some of the test objects several microspheres were molded into the same test object, to shorten the selection process.
3. A new circular plate with a diameter of 6.5 cm is cut out from the plate in the second step, with the sphere centered. The new plate is placed in the bottom

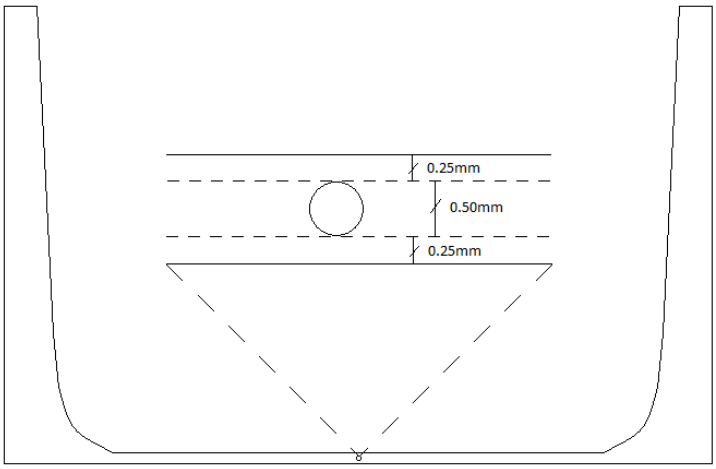

Figure 3.1: Cross section of the test object. The bottom layer is enhanced to show the all the layers from the molding.

of a cup mold and filled with approximately 70 g of liquid silicone. The bottom of the cup has a thickness of 1 mm. In this step it is important to be aware of the orientation of the plate when placing it in the mold, to ensure a vertically centered sphere.

For all these steps, it is important to use have a surplus of liquid silicone to avoid air bubbles in the plates and the final test object. In the first two steps, the plates are pressed in a hydraulic press, with a surface temperature set to 165°C for 1 minutes low pressure, followed by 17 minutes high pressure and finally 12 minutes water cooling. After the last step, the cup mold is hardened at 165°C for 100 minutes. In Figure 3.1 the cross section of the cup is sketched, the bottom layer is enhanced to show all the layers of the molding process.

Throughout this molding process good laboratory practice is critical. It is very important to clean all surfaces with isopropanol. To ensure they are dust free, they are blown clean with compressed air and always kept in a dust free cabinet. Reference cups without hollow microspheres are made with an equal procedure.

3.1.2 Removing microspheres from test objects

When the test object has been tested, it might be interesting to remove the microsphere from the test object. This is done with a scalpel and a forceps. Two or

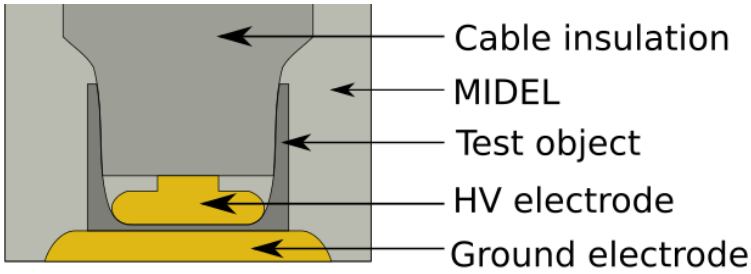

Figure 3.2: This figure shows a sketch of the electrode design, with explanation of each element.

more cuts tangent to the microsphere are made, and a forceps is used to pick the microsphere out of the test object.

3.2 Electrode design

To ensure that the test objects and especially the hollow microsphere were subject to a uniform field, the high voltage electrode had a semi Rogowski profile design [23], and the earthed electrode was plane. To reduce the risk of having other PD sources than the microsphere, the test object was submerged into a rebuilt capacitor cover filled with MIDEL. The electrode design is sketched in Figure 3.2.

To minimize the risk of having air bubbles in the MIDEL, the test object was submerged in three stages, as described in Figure 3.3 and the following procedure:

1. The test object is submerged in one smooth motion to minimize the number of air bubbles introduced to the MIDEL. The test object should be in the position shown in Figure 3.3a for 15-20 minutes, or until all the air bubbles on the bottom surface of the cup are gone.

2. Flip the test object to the position in Figure 3.3b, then submerge the HV electrode, and place it beside the test object. It is preferable to shake and stir the electrode in the MIDEL to free air bubbles between the electrode and the cable insulation. The setup should be in this position for an hour.

3. The HV electrode is now carefully moved to position 3 without lifting the HV electrode out of the MIDEL. If this is a problem, more MIDEL need to be filled into the container. Place the lid on the container to avoid pollutions entering the container.

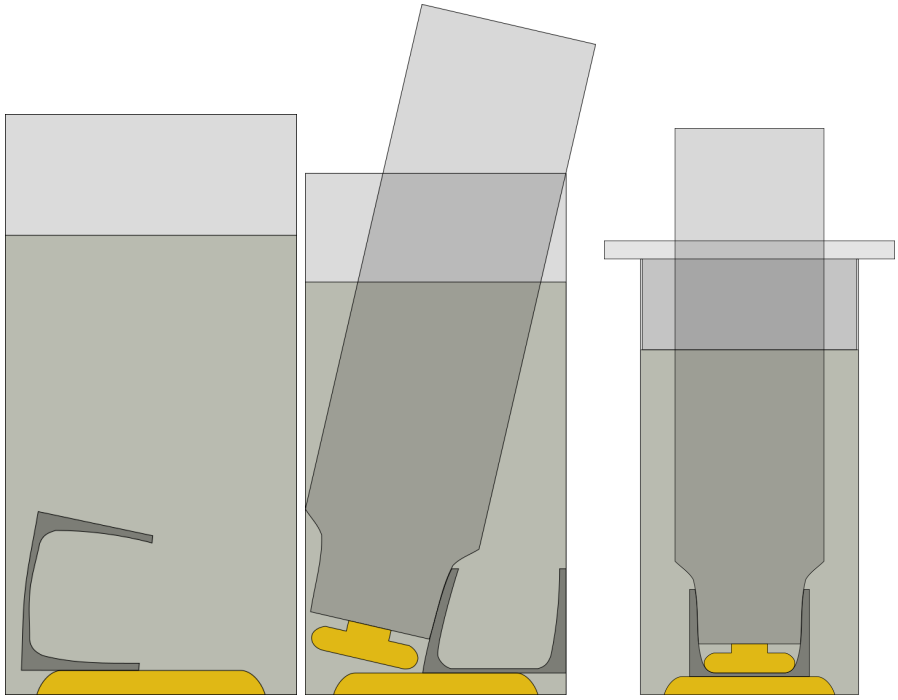

(a) Step 1 **(b)** Step 2 **(c)** Step 3

Figure 3.3: This figure explains the positioning of the test object and the HV electrode during the three steps of the submerging process.

Table 3.1: The material properties needed for the COMSOL model [24, 25, 26].

Material	Air	Glass [24]	Silicone [25]	Midel [26]
ε_r	1	4.2	2.8	3.2

3.3 Simulations

To find the field enhancement inside the microsphere, a model of a sphere in a plate was made in COMSOL. A larger COMSOL model also was built to test the field distribution around the HV electrode. The dimensions in the model is based on measurements of the test object and the test setup. The only material property needed to perform electrostatic studies is the relative permittivities, and their values are presented in Table 3.1. The relative permittivity for the glass in the spheres is not known, but assumed to be 4.2 based on the literature [24].

Table 3.2: The dimensions used for the test object in the COMSOL model.

Part	$r_{sphere,i}$	$r_{sphere,o}$	h_{bottom}	$r_{cup,i}$	$r_{cup,o}$	h_{cup}
d [mm]	0.228	0.25	0.5	22.5	33	42

Table 3.2 presents the dimensions used for the cup in the COMSOL model. The rest of the model was approximately made with Bézier curves.

3.4 PD measuring

To measure the PD activity and voltage across the test object, equipment from Omicron is used. The test circuit is constructed according to the User Manual [27], with a coupling capacitor of 800 pF. A low pass filter is used to reduce the noise. The voltage source in the first part of this work was a combination of a HV transformer and a variac, due to a broken HV amplifier. The test circuit is shown in Figure 3.4.

The test circuit was changed when the HV amplifier was repaired. Figure 3.5 shows the new test circuit. This setup makes it possible to change frequency without entering the test chamber and changing the setup. The OMICRON software is not designed for measuring low frequencies, causing error in the voltage measurements at low frequencies. Thus, the voltage measurements are assisted with a HV probe connected to an oscilloscope at frequencies lower than 1 Hz.

The Omicron system measures the voltage and this need to be calibrated. The calibration is done by applying HV to the test circuit, with a HV probe connected to an oscilloscope, the voltage over the test object is measured. The measured value is set as a target value in the software and a divider factor is calculated.

The capacitance of each test object might be slightly different, therefore it is important to calibrate the measuring system with a known charge before testing a new test object. The calibration is done by applying a charge of 20 pC from the calibrator (CAL 542), the target value in the Omicron system is set to the same value as the calibrating charge and the divider factor is found. It is good practice to apply some other charges after the calibration to check if the calibration is valid for a wider range.

The phase shift between the applied voltage and the measured discharges is found by attaching a corona source to the HV side of the test object. The corona source was a thin metal wire pointing out in the air. The phase shift is found by subtracting the phase angle of the peak of the applied voltage from the phase angle of the centre

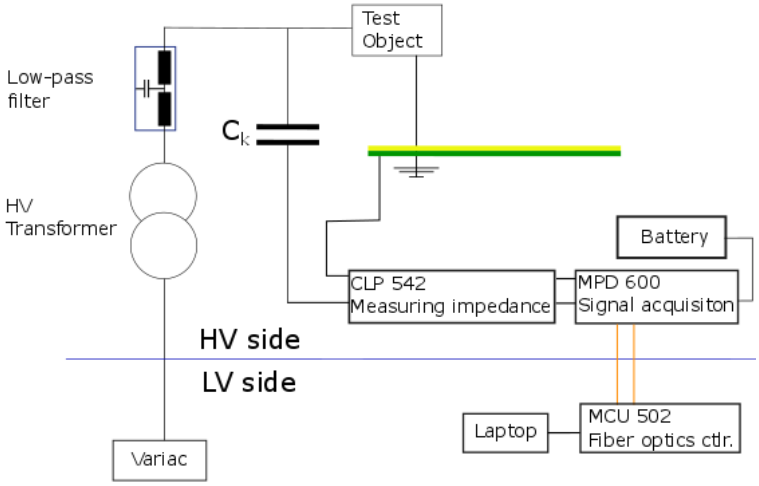

Figure 3.4: The test circuit with a transformer are constructed according to [3] and [27], with the measuring impedance in series with the coupling capacitor.

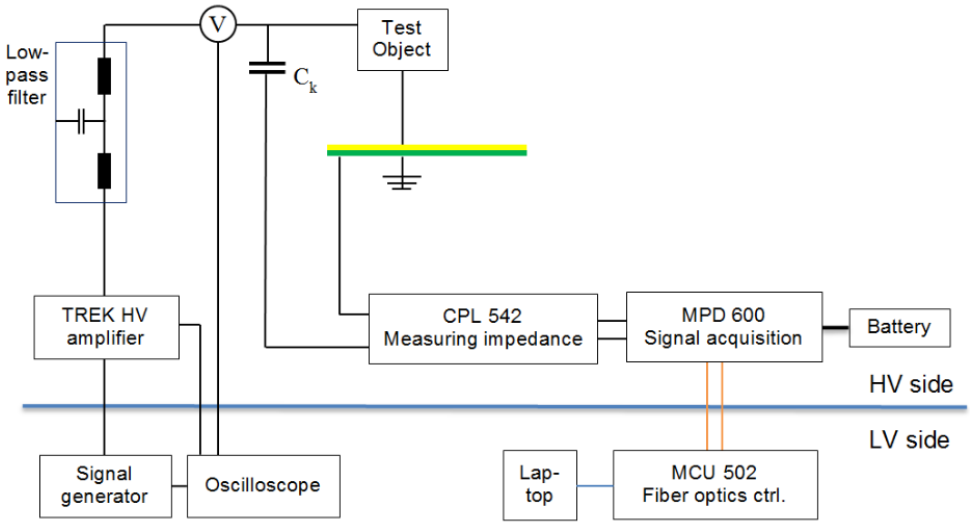

Figure 3.5: Test circuit with signal generator connected to a HV amplifier [28].

of the corona discharges. At 1 Hz and 0.1 Hz, the voltage detected can be a phase shifted sinusoidal, which need to be taken into account in the phase shift value.

Table 3.3: This table presents at which frequencies the PDIV and PDEV tests are performed, and the time duration of each voltage step at the given frequency.

f [Hz]	50.2	10	5	1	0.1	50.2
t [min]	5	5	5	10	100	5

3.4.1 PDIV and PDEV

The PDIV is found by rising the voltage until repeating PDs appear. Due to the statistical time lag explained in Theory 2.1, the voltage need to be kept constant for some time. In this experiment the voltage was kept constant for five minutes at the higher frequencies, and 600 cycles for the lower frequencies. The starting voltage level was 0.5 kV, and the voltage was incremented with 0.5 kV every fifth minute or 600^{th} cycle, until PDIV was reached. Then the voltage was decreased with the same decrement of 0.5 kV for the same time duration until all repeating PD disappeared. During the selection process of suited spheres, different time intervals was used to reduce the duration of tests. The procedure was performed for the range of frequencies presented in Table 3.3. The reason for choosing 50.2 Hz, was to avoid disturbances caused by the power grid, external 50 Hz-sources and above harmonics.

The importance of having a conditioning period before each test and how it affects the availability of the start electrons was not fully understood before late in this work. Before each test of the final test object, a conditioning period of 16.5 hours was used with 6 kV applied voltage. The tests was also performed with a grounding conditioning, where the test object was put to ground potential for 16.5 hours before testing. Before the test object was put to ground potential, the voltage was kept above PDIV.

3.4.2 Evaluating source of error in the project thesis

In the work with the project thesis [29] leading to this work, silver-epoxy was painted on the test object to avoid a surface roughness problem. This paint became brittle when it dried, and cracks formed in the paint. This was believed to be the source of the unexpected high PDs during testing. Therefore, a test object without silver-epoxy was first tested for comparison.

3.5 PD analysis

The measured PDs are analysed is several ways, both in real time and afterwards. Different methods for analysing are presented in the following.

3.5.1 PRPD analysis

The OMICRON software build real time PRPD-plot which gives the opportunity to change parameter for the plot during the tests. An important parameter to adjust, is the discharge threshold, meaning the minimum amplitude of the recorded discharges. This should be placed just below the top of the noise level. In this way no important discharge data is not lost, and files are not unnecessary large if the measurement is stream recorded. It is also possible to adjust the noise level to a higher level when exporting the data. For the test circuit used in this work, the measuring impedance is connected in series with the coupling capacitor. Thus, the PDs are detected with an opposite polarity [17]. The polarity is not inverted in this work, to be consistent with the figures produced by the OMICRON software.

3.5.2 Weibull analysis

Before doing further analysis the stream recorded data need to be exported to a Matlab-compatible data format. A random sequence of 600 periods were extracted from the data set, and further analysed. The noise was canceled by filtering the data with a threshold just above the noise level. The positive and negative PDs were analysed separately, by fitting each distribution to a 5-parameter Weibull distribution and separating the PRPD-plot with the two Weibull distributions. The scripts used in this analysis is included in the Appendix and based on [22].

3.5.3 Pulse sequence analysis

The same data used in the Weibull analysis, is further analysed with PSA in Matlab. The script are included in the appendix, several plots are produced by the script for this analysis. The cumulative distribution of both the time and voltage differences and PSA-plots for both the time and voltage differences are plotted.

PSA can also be done in the OMICRON software, the future need to be enabled in the PSA tab. The plots produced in the software show the intensity, which is not that good illustrated in the Matlab-plots.

4 | Results and discussion

4.1 Test objects

In the project thesis [29] the capacitance of the test objects was found to be $a = 48.6$ pF, which satisfied the sensitivity requirement of $C_k/a > 0.1$. From 16 measurements the mean thickness of the wall was found to be 22.2 µm, with $\sigma = 3.9$ µm. For a microsphere with outer diameter equal to 500 µm, the inner diameter becomes 456 µm. The short duration breakdown voltage was found to be 26 kV, the breakdown channel was formed 4 mm away from the sphere.

4.1.1 Estimation of PDIV and apparent charge

The breakdown strength of an air filled sphere with the diameter of 456 µm, was found to be approximately 5 kV/mm from the Paschen curve [7], when the pressure inside the sphere is assumed to be about 1 bar. The pressure inside the sphere is likely to be lower than 1 bar, due to a warm manufacturing process. From (2.4), the critical field strength was found to be 5.52 kV/mm, which is similar to the value found in the Paschen curve. Using the field enhancement factor for spheres, the PDIV voltage was found to be approximately 3.7 kV. From (2.7), the physical charge transfer was estimated to be 66 pC, with $b = 228$µm, $\Delta E = 5$ kV/mm and $\varepsilon_r = 4.2$. This charge transfer was higher than expected and probably caused by the use of a too high pressure in these calculations.

4.1.2 Evaluating source of error in the project thesis

To test if the silver-epoxy was a likely source of the high PDs in the project thesis, a test object with a microsphere without silver-epoxy paint was tested. Figure 4.1 shows an example of high PDs detected in the project thesis, at 5 kV and 50 Hz.

Figure 4.2 shows the PRPD-plots for the cup without silver-epoxy paint at different voltage levels. Discharges on the rising part of the half cycle of the applied voltage and quite constant amplitude of the upper "cloud" at 2.0 and 2.5 kV, are consistent with cavity discharges. But the same "cloud" moves forward on the phase when the voltage is decreased, which is not consistent with cavity discharges. The discharges should move forward on the phase when the voltage is increased in the case of cavity discharges, as explained in Theory 2.1.2. The discharges were not further investigated at this point, but later found to be related to metal particles in the MIDEL. The most important finding in this experiment was that no higher PDs were initiated, making the paint a likely source of the high discharges in the project thesis. Therefore, finding a new surface material was necessary.

Several surface materials were investigated and suggested as a possible solution. A semi-conduction silicone material was suggested, but no transparent materials were found. Without the transparent property, it is not possible to perform visual detection of air-filled cavities in the test objects. Therefore, this method was not tried. Salt water electrodes were also suggested. By covering the bottom of the cup with salt water and placing the test object in a brass mold also filled with some salt water, the roughness problem was avoided. But this setup did not allow the test object and the HV electrode to be submerged into MIDEL, which would increase the risk of corona and creepage current along the surface of the test object. The simplest solution was to have no conducting surface material applied to the test object. This would cause a thin layer of MIDEL to be present between the electrodes and the test object, but the layer is assumed to be very thin compared the test object. Also the roughness problem would not be eliminated, but the roughness is assumed to be small compared to the thickness of the test object. If there is an effect of the roughness, it would be most evident on the region closest to the electrodes and not affect the field strength in the spheres in a significant way. Thus, the absence of a conducting surface was chosen to be best solution for this work.

4.2 Simulations

The simulations of the test object were performed in COMSOL Multiphysics. The purpose of the simulations were to find the field enhancement in the microsphere, and also to investigate if there were other parts of the test setup experiencing high fields. First, a simulation of the bottom plate of the cup with a microsphere embedded was performed. Figure 4.3 shows the results of the simulation when the potential on the upper surface of the plate is set to 1 kV and the bottom surface has ground potential. The electric field inside the microsphere is quite evenly distributed, with a slightly weaker field in the areas closest to the electrodes. The field strength inside the

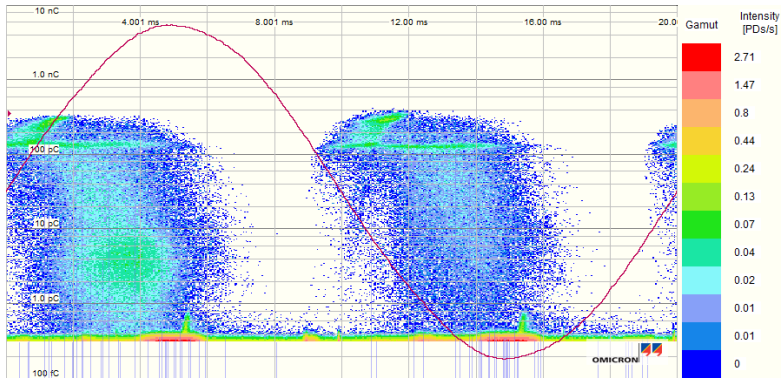

Figure 4.1: PRPD-plot from a test of a reference cup in the project thesis with V=5.0 kV [29]. This cup was expected to be PD free, due to the absence of a microsphere in it. This was not the case, the cup gave very high PDs, up to 400 pC. The PD source was believed to be the silver-epoxy, and possible cracks in the paint.

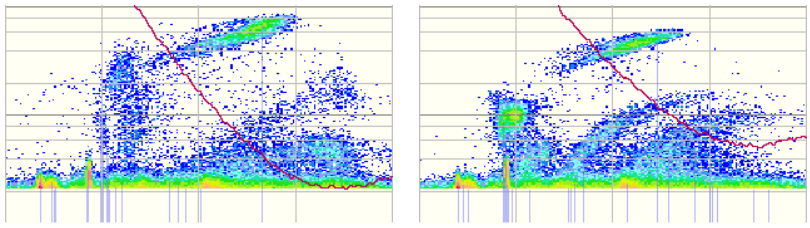

(a) 2.5 kV **(b)** 2.0 kV

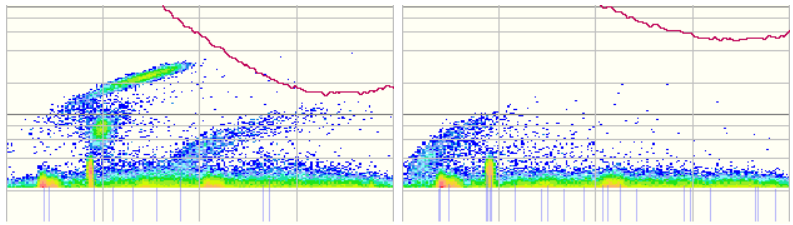

(c) 1.5 kV **(d)** 1.0 kV

Figure 4.2: These figures show extracted sections of the PRPD plot for the test on a cup with a sphere. The sections show the plot between 144° and 288° in a linear scale, 0.1 pC and 10 pC in a logarithmic scale. The plots show no higher PDs than 10 pC. Therefore, the silver-epoxy paint is likely to be the source of the high PDs in the project thesis.

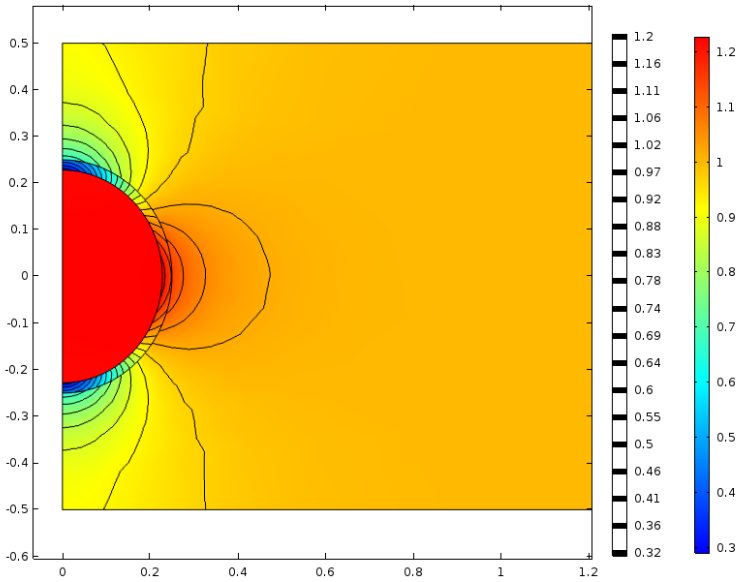

Figure 4.3: The figure shows the simulation results for the simplified model, which consists of a sphere inside a plate. The applied voltage to the upper surface of the plate is 1.0 kV and the lower plate has earth potential. The bar on the right-hand side explains the color range in the figure, the values are given in kV/mm. The lines in the figure are contour lines of the electric field.

sphere is about 1.23 kV/mm. This means that the conversion factor from the applied voltage at the HV electrode to the electric field strength inside the microsphere is $1.23\frac{\mathrm{kV/mm}}{\mathrm{kV}}$.

A simulation of the whole setup was performed, to check if other parts of the setup had high electric fields. The result from the simulation, where the potential of all parts of the HV electrode is set to 1.0 kV, is shown in Figure 4.4. This revealed that in the part where the HV electrode and the silicone cup are separated, the field strength in the MIDEL is quite high, up to 1.0 kV/mm. If an air bubble is confined in this area it is likely to have PDs initiated in this bubble. This shows how critically it is to have an air bubble free setup, especially in the region close to the electrodes.

4.3 Cup with sphere No.1

For this test the transformer was used, because the HV amplifier was still being repaired. The three first test series on the test object were performed with 5 minute time steps, the rest was performed with 2 minute time steps to reduce the duration

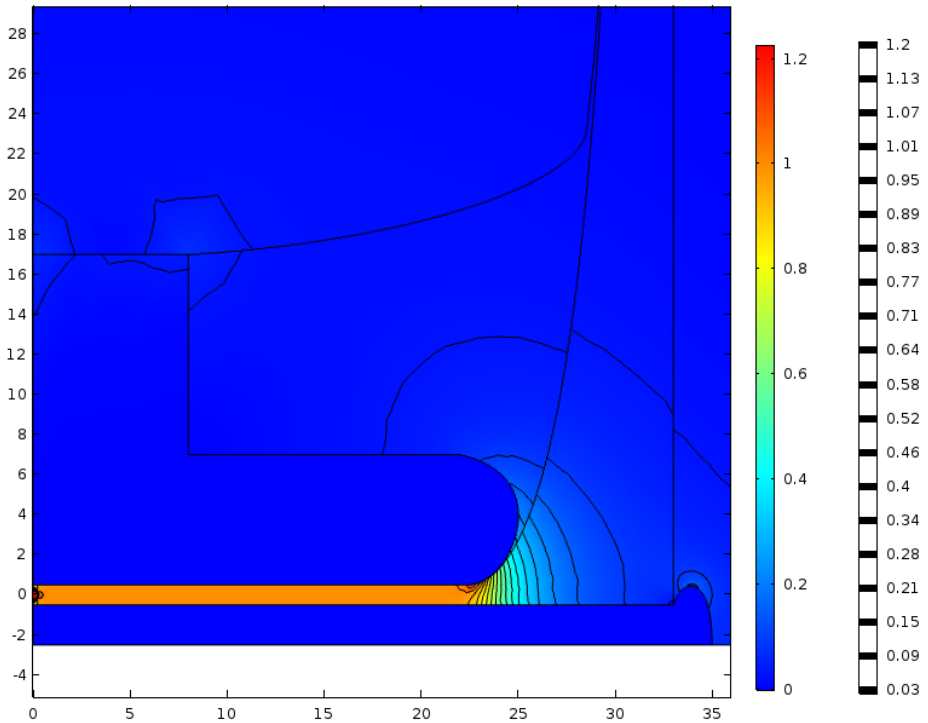

Figure 4.4: The figure shows the results from simulation of the whole test setup. All the boundaries of the HV electrode is set to 1.0 kV. The semi-Rogowski electrode is not perfectly replicated. Therefore, the field strength around the curvature might differ from the real electrode. Nevertheless, this model reveals a critical area in the setup. In the part where the HV electrode and the test object starts separating, the field strength is quite high, up to 1 kV/mm. The bar on the right-hand side explains the color range in the figure, the values are given in kV/mm. The lines in the figure are contour lines of the electric field.

of the test series. The voltage steps in the first test series were 0.25 kV, and later increased to 0.5 kV to reduce the duration of the test series.

The first test series showed non-consistency in the discharge behaviour, and differed from typical PRPD-patterns for cavity discharges. Figure 4.5 shows the development in PRPD-patterns for increasing voltage. The discharge location on the phase shifts back and forth for each voltage level, develops to different amplitudes and then totally disappear. This was first thought to be related to air bubbles in the MIDEL. The air bubbles may vanish when they are stressed by PDs and new ones might be ignited. Later these PDs were thought to be related to pollutions in the Midel, which is discussed in the following.

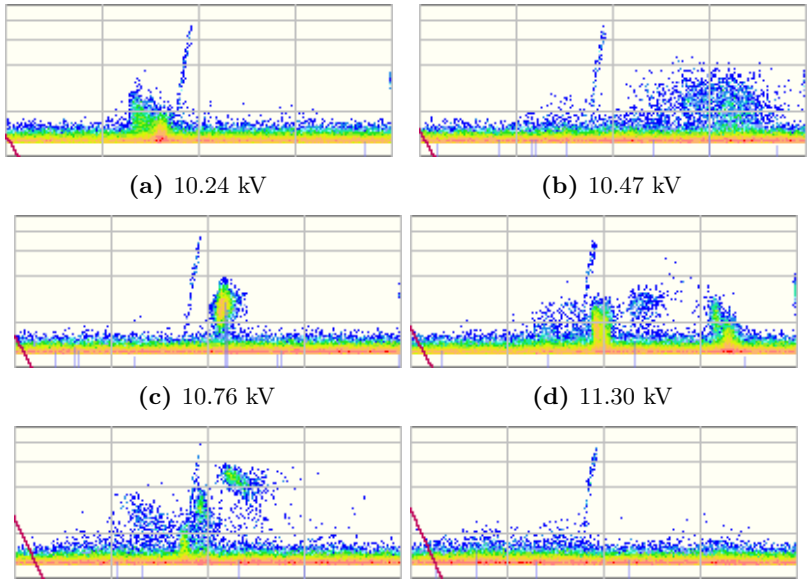

(a) 10.24 kV **(b)** 10.47 kV

(c) 10.76 kV **(d)** 11.30 kV

(e) 12.52 kV **(f)** 13.06 kV

Figure 4.5: These figures show extracted sections of the PRPD plot for the test on cup with sphere No.1. The sections show the plot between 144° and 288° in a linear scale, 1 pC and 10 pC in a logarithmic scale. The plots show a development that is non-consistent with cavity discharges. The discharges seen in the last figure are related to external noise from a heating cabinet.

4.4 Reference cup

Due to the unexpected discharges in the previous test object, a reference cup was tested to check if the PDs were related to the previous test object, or if there was an external PD source. Figure 4.6 shows PRPD-plots for both Cup with sphere No.1 and a reference cup, they all show similar patterns, which might indicate a common PD source possibly caused by pollutions in the MIDEL. In some of the test series with the reference cup, the PDs disappeared when the voltage was increased beyond PDIV. Similar patterns, as some of the ones recorded here, are found in the literature [30, 16], and may be related to a floating metallic particle or a foil particle with a sharp edge.

Based on the discharges found when testing the reference cup and findings in the literature, it was decided to change the MIDEL. When emptying the container a couple of small flakes of the silver-epoxy paint were found. The container and the electrodes were completely disassembled and thoroughly cleaned with isopropanol.

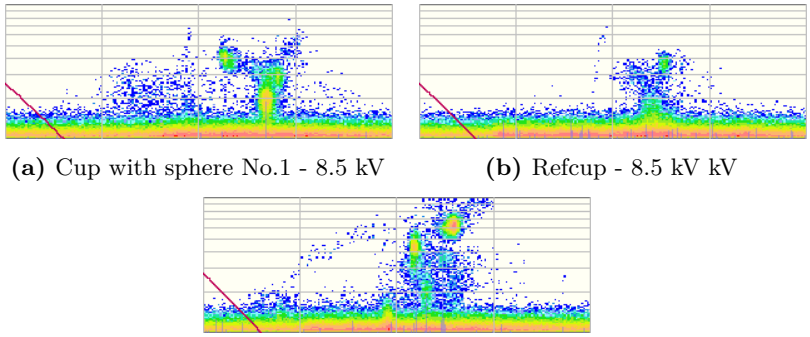

(a) Cup with sphere No.1 - 8.5 kV **(b)** Refcup - 8.5 kV kV

(c) Refcup, redo - 9.0 kV

Figure 4.6: These figures show extracted sections of the PRPD plots for the tests comparing cup with sphere No.1 with a reference cup. The sections show the plot between 144° and 288° in a linear scale, 1 pC and 10 pC in a logarithmic scale. The plots show a similar pattern for different test objects at similar voltage.

When the setup was assembled, all the parts were lowered into the new MIDEL in such a way that the chance for introducing air bubbles in the MIDEL was small. An axial hollow bolt was used when the ground electrode was lowered, to free the air captured beneath the ground electrode and to avoid it from being released later.

4.5 Cup with sphere No.2

The tests on a new test object with a new hollow microsphere is described in this section, the test object was called Cup with sphere No.2. During the test of this test object the HV amplifier was returned, allowing tests at frequencies different from 50 Hz.

In some of the tests at 50 Hz with the transformer and at 50.2 Hz with the HV amplifier, a strange phenomena was observed. The amplitude of the recorded discharges varied periodically between 3 pC and 9 pC with a period of about 14 seconds. There was a month difference between the first and the last observation of this type of discharges. This type of discharges is not consistent with cavity discharges, and the source for the discharges was not further investigated. The periodically change in discharge size is shown in Appendix B. Figure B.1 shows a PRPD plot from such a situation and Figure B.2 shows the varying maximal amplitude of the discharges with a time scale, the period for is at about 14 seconds. The test object was tested at different frequencies without showing consistency in the measured discharges.

Table 4.1: This table presents the phase shift between the measured voltage and the measured discharges, caused by the frequency dependency of the measuring impedance.

f [Hz]	10	5	1	0.1
$\Delta\varphi$ [°]	3	3	-5	-55

One month after the first test, typical PD patterns for cavities was observed at several frequencies. But the tests was terminated, due to the other present PD sources and the risk of changed properties of the silicone cup. The long time of submerging might change the permittivity of the silicone and the field distribution, due to ingress of MIDEL.

4.6 Phase shift due to measuring impedance

The phase shift between the applied voltage and the measured PDs are presented in Table 4.1. The voltage detected by the measure equipment, can be shifted from a sinusoidal shape, which also need to be compensated for. This phase shift can vary for each test series and need to be evaluated when exporting the data.

4.7 Cup with 5 spheres

To speed up the process for finding spheres suited for further testing, several spheres was molded into the test objects. This section describes the findings from tests on a test object with 5 spheres. The test object was first tested at 50.2 Hz, with voltage steps of 0.5 kV, starting at 0.5 kV, and 2 minutes at each step. At the very end of the test at 6.0 kV, repeating PDs appeared. The voltage was further increased to 6.5 kV, to have more discharges recorded.

The PRPD-plots of the PD events, which are shown in Figure 4.7, indicated cavity discharges with good start electron availability. The PDs appeared on the rising part of the voltage cycle. They had a quite constant amplitude and were spread at a decreasing part of the period with decreasing applied voltage. This is consistent with the *abc*-model. Figure 4.7a shows a PRPD-plot at 6.5 kV, in the cloud of PDs it is possible to see some areas with a larger intensity, especially for the negative PDs. This is very consistent with the *abc*-model.

A PD will occur when the electric field inside the sphere exceeds a critical value and a start electron is available. According to the *abc*-model the voltage will be

Table 4.2: Repetition rate from first test on Cup with 5 spheres at 50.2 Hz, for PDs with a greater amplitude than 3 pC.

V [kV]	6.5	6.0	5.5	5.0	4.5	4.0	3.5	3.0	2.5	2.0
n [PDs/period]	9.7	8.6	7.7	6.7	5.8	4.8	4.0	3.2	2.3	1.8

reduced to a remnant voltage. The difference between the ignition voltage, U_{s0}, and the remnant voltage, U_{r0}, should theoretically be constant. In Figure 4.7 all the clouds of discharges have a quite constant amplitude, indicating a quite constant difference between U_{s0} and U_{r0}. When the field is increased above $E_{critical}$, the repetition rate of the PD events should increase when the applied voltage is increased, and decrease when the voltage is decreased. This is consistent with the results from this test object as shown in Figure 4.7 and Table 4.2. For the voltage levels shown in Figure 4.7, the repetition rate is close to an even number, which means that the number of PDs for each half cycle is close to an integer. This integer number coincides with the number of more intense areas in the clouds. Compared to Figure 2.2, the more intense areas can be related to a specific place on the phase, where the voltage across the cavity reaches U_{s0}. Because the PDs are initiated close to U_{s0}, there must a good availability start electrons once the PD activity has started.

Investigating the repetition rate at the different voltage levels, it is found that the number of PDs per half cycle is decreased with about one for every second voltage step. Indicating that the difference in the applied voltage between U_{s0} and U_{r0} is about 1 kV. Using the relation between the applied voltage and the field strength inside the cavity found in the simulation. The change in the field strength inside the sphere during a PD, ΔE_{cav} is about 1.23 kV/mm, which is 1.74 kV/mm in peak value. Compared to the breakdown strength of about 5 kV/mm found in the Paschen curve at 1 bar, this value is much lower. The difference is most likely caused by a much lower pressure than 1 bar in the sphere. The spheres are most likely produced in a very warm process, reducing the pressure in the spheres when they are cooled. Using the Paschen curve the pressure inside the sphere is found to be 0.18 bar. This value is confirmed with (2.4), giving $E_{critical} = 1.74$ KV/mm with $p = 18$ kPa and $d = 456$ µm. From (2.7) the charge transfer was found to be 23 pC with $b = 228$ µm, $\varepsilon_r = 4.2$ and $\Delta E = 1.74$ kV/mm. These values are more plausible. The difference between the physical charge transfer and the apparent charge is large, which indicate losses from the discharge site to the terminals of the test object [6].

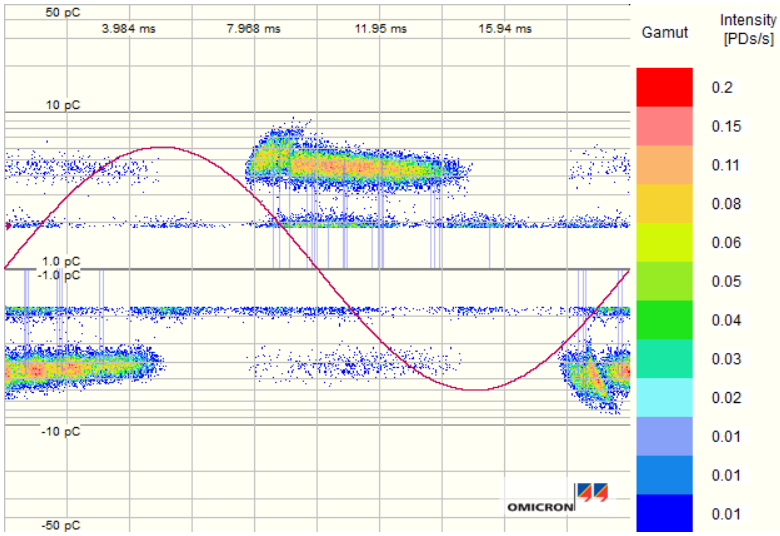

(a) Cup with 5 spheres - 6.5 kV

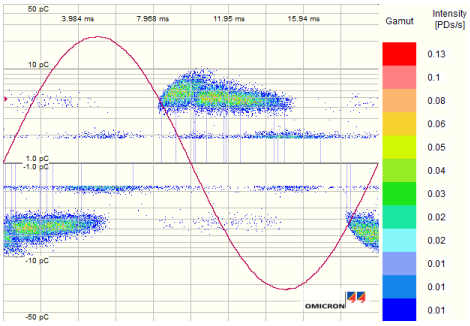

(b) Cup with 5 spheres - 4.5 kV

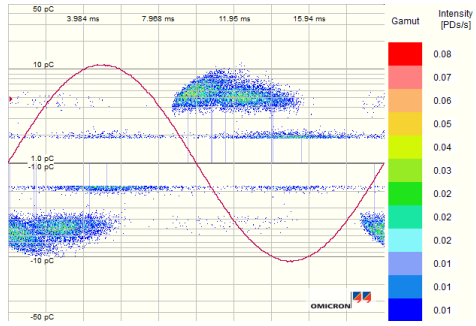

(c) Cup with 5 spheres - 3.5 kV

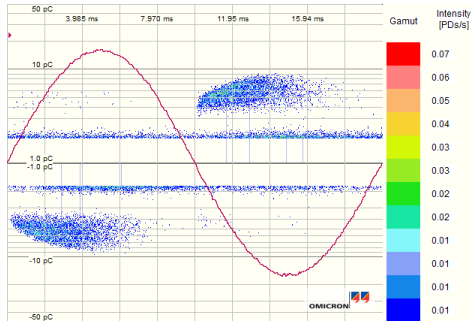

(d) Cup with 5 spheres - 2.5 kV

Figure 4.7: These figures show the PRPD plots from the first test on Cup with 5 spheres at 50.2 Hz. The amplitude of the discharges is quite constant and the repetition rate is decreasing with decreasing voltage.

4.7.1 Test are dependent on the history

The test object was further tested and gave patterns very similar to the ones in the first test series. But the history of the test object was found to be important, and the PDIV was found to be very dependent of the initial condition. After the first day of testing, the HV side of the test object was grounded with an earth rod over night. The first test the the next day had PDIV at 7.5 kV and the second test had PDIV at 3 kV. There was a short grounding period between the first and the second test. The same procedure was performed the following night and day, then the PDIV for the first test was 7.0 kV and the second test had PDIV at 2.5 kV.

The difference in the first and second PDIV-test, is caused by a memory effect in the test object. When the test object has been at earth potential for a long time, the weakly trapped charges can be trapped in deeper traps, which makes it harder to free them [6, 5]. The charges may also be recombined due to E_s. All the drifting charges are also probably trapped or recombined. So the start electron either need to be generated by radiation or released from deeper traps, of which the generation rate increases with increasing applied voltage. PDIV at similar voltage levels might indicate that the start electrons are caused by detrapping of electrons.

When the test object had been at ground potential only for a short time, PDIV was consistently at about 3 kV. The big difference in PDIV for long and short earthing must be related to the available start electrons. For the short grounding duration the start electron availability was good in the PDIV-tests, due to the consistency of PDIV for the tests. The repetition rate was lower than 4 PDs/period for all the tests, meaning PDs was initiated soon after $E_{critical}$ was exceeded. The start electrons were probably weakly trapped in the cavity wall, and then untrapped by the applied field. The start electrons may also have been drifting inside the sphere.

The first PD of a new polarity was slightly higher than the other discharges, indicating a good availability of start electrons. It also indicates that the field due to the surface charges was small compared to the applied field.

4.7.2 Consistency at different frequencies

The test object was further tested at different frequencies. The shape of the discharges in the PRPD-plot, number of PDs/period and PDEV was consistent for the frequencies tested. Table 4.3 present the repetition rate of the discharges at 2.5 kV for different frequencies. The repetition rate at 1 Hz is higher than the rest, this is most likely to be caused the longer test duration, which gave a higher noise to cavity discharge ratio. At 0.1 Hz it was too much noise to determine the repetition rate,

Table 4.3: This table presents the repetition rate at 2.5 kV for the different frequencies tested at Cup with 5 spheres. The test at 0.1 Hz had to much noise to determine the repetition rate.

Frequency [Hz]	100.4	50.2	10	1
n [PDs/period]	2.6	2.4	2.5	2.9

but it was possible to observe when the PD occurred in the PRPD-plot. Though it was hard to determine the PDEV due to the noise.

The PDIV was varying for the tests and were found to be dependent on the history. But the PDEV was very consistent for all the tests. For all of the tests PDEV was found to be 2.0 kV, at 0.1 Hz the noise made it hard to determine. This parameter should not be dependent on the history. Once repeating PDs are present, the field strength should be determining when the PDs extinguish. This property makes this parameter well suited for determining the field strength at the site of the sphere. Therefore, this parameter will be important if the spheres are to be tested in field grading material.

4.7.3 Separate testing of the spheres

Due to the consistency of the tests, the spheres from this test object was decided to be separately investigated. Thus, the spheres was picked from the test object and separately molded into new test objects. During this process one of the spheres broke, when it was picked out of the test object. The method of picking spheres out of the test objects should therefore be improved. A possible solution can be to cut out a small piece of silicone containing the sphere, and then put the piece in a liquid dissolving only the silicone, but not the glass sphere.

The new test objects, each contained one of the previously tested spheres, was tested at 50.2 Hz. The tests were normal PDIV-PDEV tests with step duration of 2 minutes. None of the tests showed any PD activity. Therefore, the voltage was kept at 10 or 11 kV for an hour for each of the new test objects. This voltage level was well above the PDIV for Cup with 5 spheres at all conditions, but still no PD activity.

There is a 20 % chance that the source for the PD activity in Cup with 5 spheres was the sphere that broke. Another explanation for the absence of PD activity in there tests are that the orientation of the sphere has changed in the second molding process. As shown in Figure 2.5, charges are located at the inner surface closest to the electrodes after a PD. If the charges are trapped here after the PD event, they

can be detrapped if a strong enough field is applied. But if spheres are shifted 90° in the new test object, compared to the original orientation, the charges may not be detrapped by the applied field.

4.8 Cup with 5 spheres No.2

A new cup with 5 spheres was tested to find spheres with results suited for further testing. This test object had some imperfections in terms of air bubbles in the wall, which could be a possible PD source. But the test object was still tested while other test objects were produced. The tests were performed with voltage step duration of 2 min at 50.2 Hz

This test object had PDIV at 9.0 kV in the first test, 9.5 kV in the second and third test, all these tests had similar patterns in the PRPD-plot at inception. Figure 4.8 shows the PRPD-plot at PDIV from the second test. The discharges have a high amplitude compared to the estimated value and the results from Cup with 5 spheres. Also there are few discharges at such a high voltage level, compared to the previous results.

Figure 4.9 shows the PRPD-plot from the forth test at 9.0 kV after the voltage had been risen above PDIV and stepped down to PDEV. In this test, PDIV was 8.5 kV, PDEV was 8.0 kV and the voltage was risen to 11.0 kV to explore the development beyond PDIV. The plot does not shows great symmetry for the positive and negative PDs, this can also be seen in Figure 4.8. This might indicate that the PD source is not centered between the electrodes or that the surface of the PD source are not even, the air bubbles in the wall were therefore assumed to be the PD source. A centered discharge source will give symmetric discharges [5]. Due to the high discharges and the non consistency with Cup with 5 spheres, the tests on this test object was terminated after five tests at 50.2 Hz.

4.9 Cup with 5 spheres No. 3, 4 and 5

All the tests in this section was performed at 50.2 Hz. When Cup with 5 spheres No. 3 was tested some small PDs with a maximum charge amplitude of 3 pC was observed at 7 kV. The voltage was kept at this voltage level to observe if there was a development. The PDs shifted forward on the phase, and then disappeared. The voltage was further risen to 10 kV, without observing any PDs. The test on this test object was therefore terminated.

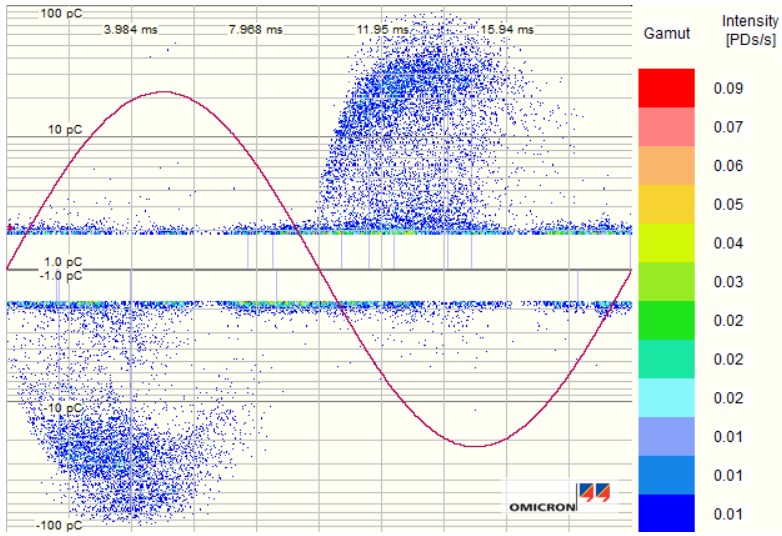

Figure 4.8: PRPD-plot at PDIV = 9.5 kV from second test on Cup with 5 spheres No.2 at 50.2 Hz.

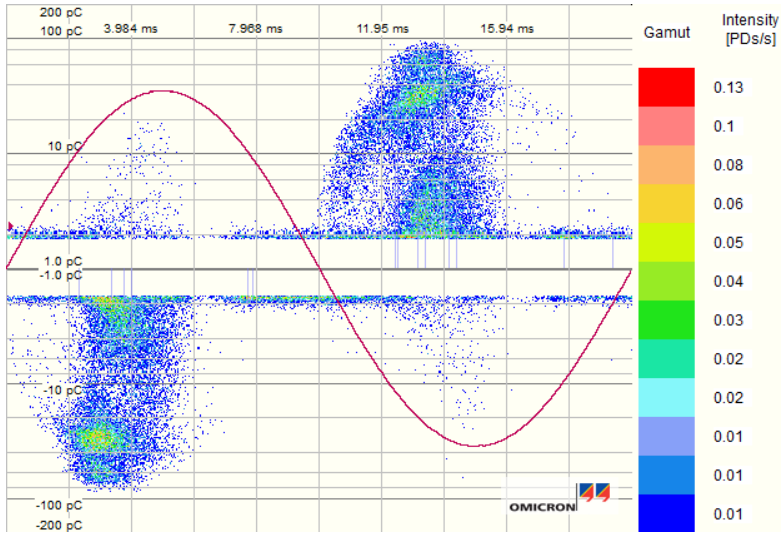

Figure 4.9: PRPD-plot at 9.0 kV from forth test on Cup with 5 spheres No.2 at 50.2 Hz.

The tests on Cup with 5 spheres No. 4 gave similar results as Cup with 5 spheres No. 3. In the first and second test, the PDIV was 6 kV with a maximal discharge amplitude of 3 pC. In the second test the voltage was lowered below PDEV and then risen again, then the PD first appeared at 8.5 kV with a maximal amplitude of 4 pC. Due to this inconsistency a third test was performed. In the third test PDIV was found to be 10 kV, with maximal amplitude of 4 pC. The voltage was kept at this level for an hour to check the continuity of the discharges. The discharges first disappeared, then reappeared after 40 minutes and disappeared after 6 more minutes. Due to the inconsistency the tests on this test object was terminated.

The test on Cup with sphere No. 5 showed no PD activity in the PDIV test, when the voltage level reached 10 kV the voltage was kept at this voltage for an hour. No PD activity was recorded in this test. Thus, the test was terminated. The absence of discharges in this test shows that the setup is PD free and the recorded discharges are caused by the test objects.

4.10 Cup with 6 spheres

This section describes the tests on Cup with 6 spheres, this is a test object which showed promising results for further testing.

4.10.1 First tests

The first test on Cup with 6 spheres was performed at 50.2 Hz with time steps of 2 minutes. At 8.0 kV, PDs appeared with a maximal amplitude of 3 pC, these PDs were present up to 10.0 kV. At 9.0 and 9.5 kV, some discharges with amplitudes between 5 and 9 pC appeared. At 10.50 kV, no PDs were recorded. Higher discharges appeared at 11 kV, the amplitude were between 5 and 10 pC and similar to the ones shown in Figure 4.10a, but these PDs disappeared after some seconds.

At 11.5 kV PDs similar to the discharges observed at 11 kV, the PRPD-plot is shown in Figure 4.10a. The plot is very similar to the results from Cup with 5 spheres, and has good fit to the *abc*-model. The development in the PRPD-plots in Figure 4.10 and the repetition rates presented in Table 4.4, shows that the availability for start electrons are poor. In Figure 4.10a it is possible to see a small "rabbit-ear". At 10.0 kV the "rabbit-ear" lasts to the peak of the applied voltage, as shown in Figure 4.10b. The maximal amplitude is in this case 50 pC and the repetition rate is 4 PDs/period. The reason for the high amplitude is a combination of relatively high voltages, poor availability of start electrons and surface charges. As explained in the

Table 4.4: This table shows the repetition rate for the PDs in the first test on Cup with 6 spheres, where the threshold is set to 3 pC. The table only contains every second measurement, due to readability.

V [kV]	11.5	10.5	9.5	8.5	7.5	6.5	5.5	4.5	3.5
n [PDs/period]	9.1	5.8	2.4	0.25	0.16	0.16	0.13	0.09	0.01

Theory with Figure 2.6b, the field due to surface charges has the same direction as the applied field after the first change of polarity of the voltage after a PD event. When the availability of start electrons is poor, the field inside the cavity can become large before a PD is initiated, giving high discharge amplitudes. The field inside the cavity should have close to a linear relationship to the applied voltage if the surface charges are constant, but some of the surface charge can recombine and cause the Poisonnian field to decrease. Due to the poor availability of start electrons, the PDs can appear after the peak of the applied voltage, as long as the field is strong enough to initiate a PD. The concentration of PDs is highest close to the peak of the voltage in Figure 4.10c. This is most likely a result of the field inside the sphere being strongest here, and the detrapping rate is therefore highest. Figure 4.10c and 4.10d show that the amplitude of the discharges have a great resemblance to the amplitude of the applied voltage, taking into account that the scale for the discharge amplitude is logarithmic and the scale for the voltage is linear. The lack of start electrons explains the relatively high PD amplitude for the lower voltages, compared to the PD amplitude at PDIV.

In the two following tests the PDIV was at 5.5 kV and 6.0 kV. The PRPD-plots were very similar for these tests, Figure 4.11 presents the PRPD-plot from the second test at 5.5 kV. The maximal amplitude in these tests were at about 30 pC, which is consistent with the maximal amplitude in Figure 4.10d. In the forth test the voltage was risen to 14.5 kV without having higher PDs. Based on these varying results and the memory effect, in terms of trapping rate and waiting time for a start electron, it was decided that the test objects should be conditioned. With a conditioning period, all the tests objects were assumed to reach a steady state condition and all the tests would have the same initial condition. The conditioning period was decided to be 16.5 hours, both of practical reasons and the assumption of reaching a steady state condition during this period. The average waiting time for a start electron for a cavity of this size is about 3 hours [6]. The conditioning voltage was decided to be 6.0 kV, which was a voltage where PDs had been detected in the earlier tests.

During the conditioning periods, the PRPD-plots were built. Every 10^{th} minute a five minute recording began, the next five minutes no recording was performed. In the first conditioning period, no PDs were detected in the first 10 hours. After 10 hours, PDs with an maximal amplitude of 6 pC was observed. The repetition

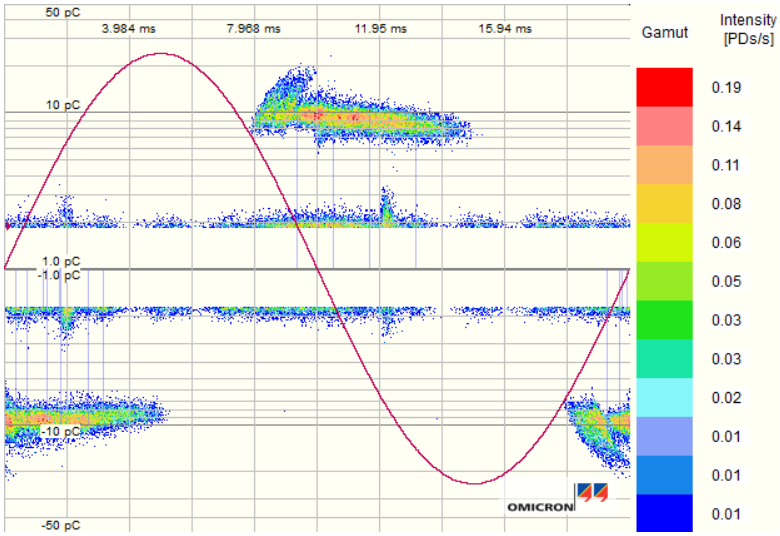

(a) 11.5 kV

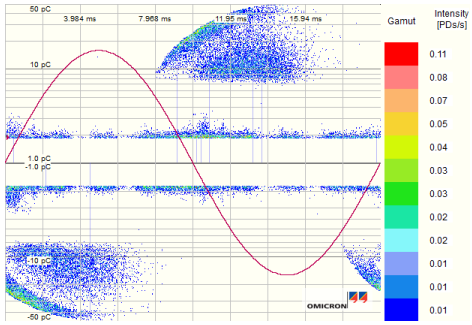

(b) 10.0 kV

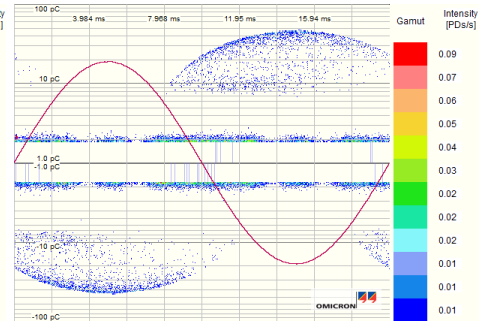

(c) 9.0 kV

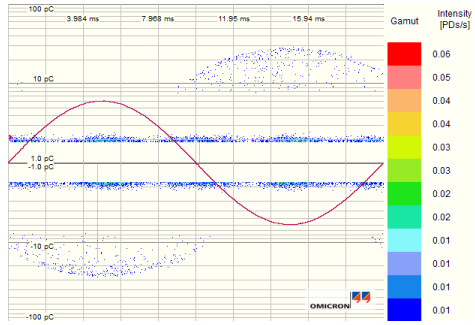

(d) 5.5 kV

Figure 4.10: These figures show the PRPD plots from the first test on Cup with 6 spheres. The first two plots have a range from 1 to 50 pC, the two last plots have a range from 1 to 100 pC.

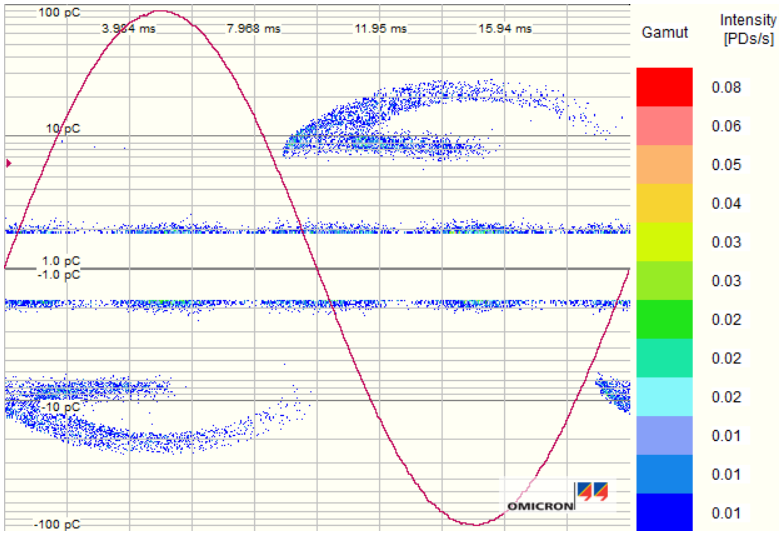

Figure 4.11: This figure shows the PRPD-plot from the second test on Cup with 6 spheres at PDIV = 5.5 kV.

Table 4.5: This table presents selected repetition rates for the first conditioning of Cup with 6 spheres. The rates are from the same recordings as in Figure 4.12.

t [hours]	10	16	16.5
n [PDs/period]	7.8	11.9	21.4

rate for the PDs in this case, was calculated by subtracting the noise from the total number of PDs, earlier "noise-plots" had about 17 000 PDs. The repetition rates are presented in Table 4.5. A section of the PRPD-plot recorded after 10 hours are presented in Figure 4.12a, it is possible to see four more concentrated areas, which confine with the repetition rate. During the night the battery for the measuring equipment went flat. The first PRPD-plot recorded after the battery was changed, is presented in Figure 4.12b. It appears to have been a development with higher discharges up to 20 pC. The repetition rate has also increased to 11.9 PDs/period, indicating the ignition of another discharge source. In the last PRPD-plot recorded, there was a further development, as shown in Figure 4.12c. Another PD source seem to be ignited, and the increase in the repetition rate supports this suspicion, with about 5 more PDs per half cycle.

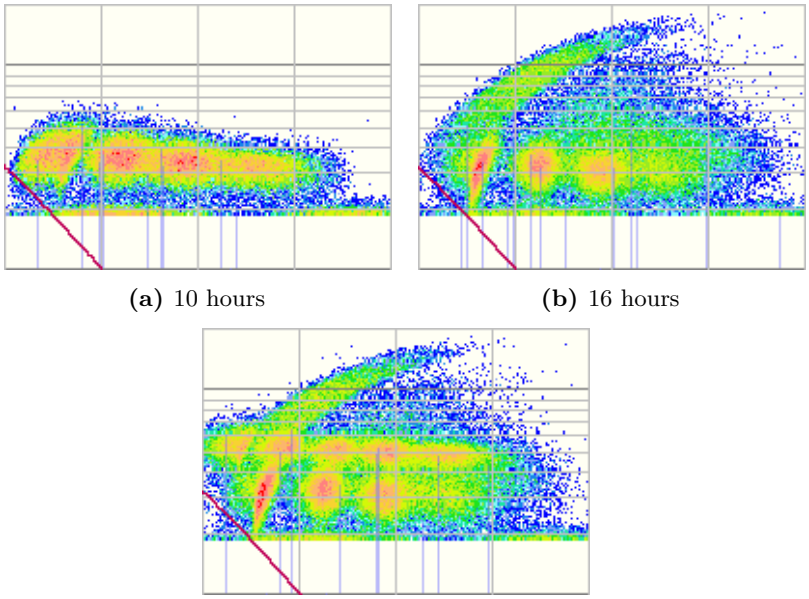

(a) 10 hours **(b)** 16 hours

(c) 16.5 hours

Figure 4.12: These figures show extracted sections of the PRPD-plots for the first conditioning on Cup with 6 spheres. The sections show the plot between 144° and 288° in a linear scale, 1 pC and 20 pC in a logarithmic scale. The plots show a development in the number of PDs and the amplitude, indicating several PD sources.

4.10.2 PDIV - PDEV test with voltage conditioning

The test object was now test at the frequencies in Table 3.3. Before each PDIV - PDEV test, the test object was conditioned for 16.5 hours with an applied voltage at 6 kV. For the four first tests the PRPD plots were similar, as shown in Figure 4.13, and significantly different from the noise level. The plots from the two lasts tests, show two "clouds". The cloud with lowest discharge amplitude is most intense, which indicate two separate discharge sources. If there had been one discharge source, the first discharge would have the highest amplitude due to surface charge and lack of start electron. Therefore, the "cloud" with highest amplitude would be most intense. In Figure 4.13f both the "clouds" have discharges after the peak of the voltage, indicating poor availability of start electrons. If there was one PD source the "cloud" with lowest amplitude should stop at the peak of the applied field, as in Figure 4.11.

Table 4.6 presents different parameters found from the PD-data. The repetition rate is close to 2 PDs/period for the three first tests, which is consistent with the

Table 4.6: Derived parameters for voltage conditioned tests on Cup with 6 spheres. The noise is filtered at 3 pC except 0.1 Hz and 50.2 Hz redo the noise limit was set to 2.5 pC

f [Hz]	50.2	10	5	1	0.1	50.2, redo
PDIV [kV]	2.0	2.0	2.0	2.5	3	2.5
PDEV [kV]	2.0	2.0	2.0	2.0	2.0	2.5
n [PDs/period]	2.0	2.0	1.9	2.9	3.1	2.2
q_{max} [pC]	9.8	10.4	11.4	12.6	16.3	16.6
q_{avg} [pC]	5.6	6.0	6.6	6.7	5.1	5.9

PRPD-plots. The tests at 1 Hz and 0.1 Hz had repetition rates above 2, this can be caused by PDIV above E_{crit} or several PD sources. At 0.1 Hz it appear to be two PD sources in the PRPD-plot as shown in Figure 4.13e, this can also be the case at 1 Hz. The following test at 50.2 Hz have a similar PRPD-plot to 0.1 Hz. Even if the repetition rate indicates only one PD per half cycle, the PRPD-plot reveals that is likely two PD sources with poor availability of start electrons.

The PDIV and PDEV show a good consistency in these tests. The PDEV is constant at 2.0 kV, except from the redo test at 50.2. In this test the PDEV was 2.5 kV which only is one step above 2.0 kV and not a significant difference. The PDIV is a bit higher for the three last tests. For the two lowest frequencies the increase in PDIV can be related to the increase in the test duration at each step and thereby an increased probability of trapping and recombination after the conditioning. The consistency in PDEV makes this a parameter well suited for further testing.

4.10.3 Weibull analysis of voltage conditioned tests

Table 4.7 and 4.8 presents the parameters found when the PD-distributions at PDIV was fitted to a 5-parameter Weibull distribution. There is a good correspondence between the parameters found for the positive and negative PDs. The biggest difference is at 1 Hz where $p_p = 0.5352$ and $p_n = 0.0910$. The separation in the negative distribution caused a large difference in the β-values, $\beta_{n1} = 12.0759$ and $\beta_{n2} = 4.0959$, due to few data points in the lower distribution the confidence interval is large for this value. In Appendix A, the cumulative distribution with a fitted 5-parameter Weibull distribution and Weibull separated PRPD-plot for the positive PDs is presented for each frequency. The plots are very similar for the positive and the negative PDs. All the β-values are within the range for void discharges found in the literature [20]. The fitted Weibull distributions generally show a quite good fit

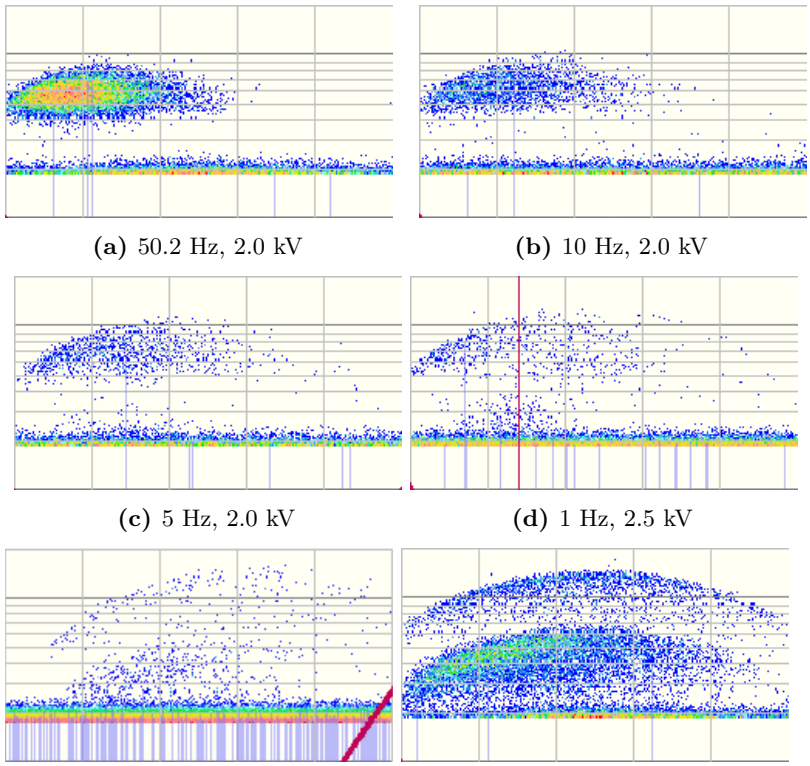

(a) 50.2 Hz, 2.0 kV

(b) 10 Hz, 2.0 kV

(c) 5 Hz, 2.0 kV

(d) 1 Hz, 2.5 kV

(e) 0.1 Hz, 3.0 kV

(f) 50.2 Hz, Redo, 2.5 kV

Figure 4.13: These figures show extracted sections of the PRPD-plots from the voltage conditioned PDIV-tests on Cup with 6 spheres. The sections show the plot between 180° and 360° in a linear scale, 1 pC and 20 pC in a logarithmic scale. At 0.1 Hz the plot is taken from the negative PDs, which is rotated and flipped, due to a large phase shift. The symmetry between the positive and the negative PDs in the PRPD-plot is good.

to the PD distributions. At 10 Hz and 0.1 Hz the lower tails of the distribution does not have a good fit, most likely because there are few discharges at the tails.

4.10.4 Pulse sequence analysis of voltage conditioned tests

Voltage differences

Figure 4.14 shows two examples of PSA-plots at PDIV for the test on 50.2 Hz and 50.2 Hz, redo. It has earlier been showed that one PD source are present at 50.2 Hz and two PD sources are present at 50.2 Hz, redo. In Figure 4.14a most of the differences are plotted in the second and forth quadrant, meaning that the voltage change polarity between most of the PDs. There is a few PDs in the first and the third quadrant, meaning that it probably has been two discharges in some of the half cycles. The maximal difference is the peak to peak value, which was 5.7 kV in this case. Most of the differences are at about 3 kV, indicating PDs on the rising part of the voltage half cycle, which is confirmed in Figure 4.13a.

In Figure 4.14b there are six concentrated areas in the plot. The two most intense areas are the same as in Figure 4.14a, but with a higher amplitude. The maximal difference in this case is 7.1 kV. In the most area the differences vary between 4 and 7 kV, indicating half a period between the following discharges and PDs on the rising part of the half cycle and up to the peak. This is confirmed with the most intense area in Figure 4.13f.

The other areas consist of points with a small and a large difference. These points are either a result of two discharges in the same half cycle of the voltage and one in the other half cycle or one of more periods between following PDs. For instance can the area with large positive ΔV_{n-1} and small positive ΔV_n, a result of a PD in the negative half cycle with two PD in the following positive half cycle, or two following PDs in the positive half cycle with one or more periods in between. These areas do not contain as many data points as the two most intense areas, indicating a sporadic appearance of the two discharges per half cycle and the possibility of not having PDs in each half cycle. This is also indicated with the repetition rate of 2.2 PDs/period and Figure 4.13f. The cumulative distributions, which are included in Appendix C, also supports these findings.

Table 4.7: Parameters for a 5-parameter Weibull distribution fitted to the positive PDs at PDIV. The parameters are given with their lower and upper confidence interval.

f [Hz]		p_p		α_{p1}		α_{p2}		β_{p1}		β_{p2}	
50.2	Est	0.3367		6.5045		5.4816		8.0600		10.9091	
	Conf	0.2056	0.4679	6.2257	6.7832	5.3933	5.5700	6.5694	9.5506	9.6744	12.1438
10	Est	0.2287		7.5610		6.0171		7.3778		8.3093	
	Conf	0.0742	0.3832	6.9627	8.1593	5.8677	6.1665	5.1442	9.6115	7.4579	9.1607
5	Est	0.5161		7.8022		6.2424		6.1122		8.0237	
	Conf	0.1935	0.8387	7.1635	8.4408	5.8798	6.6050	4.6875	7.5369	5.6034	10.4440
1	Est	0.5352		8.3817		6.1657		4.4901		4.7869	
	Conf	0.2203	0.8501	7.4720	9.2915	5.6918	6.6396	3.3400	5.6401	4.0214	5.5525
0.1	Est	0.3723		9.1403		3.6849		2.6867		5.0083	
	Conf	0.3236	0.4209	8.5719	9.7088	3.5911	3.7788	2.3629	3.0104	4.5811	5.4355
50.2, Redo	Est	0.1725		11.2091		4.5133		5.5668		4.6683	
	Conf	0.1385	0.2064	10.7016	11.7165	4.4132	4.6134	4.2786	6.8549	4.3055	5.0310

Table 4.8: Parameters for a 5-parameter Weibull distribution fitted to the negative PDs at PDIV. The parameters are given with their lower and upper confidence interval.

f [Hz]		p_n		α_{n1}		α_{n2}		β_{n1}		β_{n2}	
50.2	Est	0.2762		6.7961		5.6631		6.9890		9.8507	
	Conf	0.1469	0.4055	6.4521	7.1402	5.5534	5.7728	5.8235	8.1545	8.7231	10.9783
10	Est	0.4433		7.2349		5.9080		6.3482		8.9847	
	Conf	0.2289	0.6577	6.8639	7.6060	5.6374	6.1787	5.5316	7.1648	7.1556	10.8139
5	Est	0.4121		7.9776		6.3903		5.8593		7.2714	
	Conf	0.0194	0.8048	6.9779	8.9773	6.0362	6.7444	3.8712	7.8473	5.3827	9.1601
1	Est	0.0910		10.7064		7.0794		12.0759		4.0959	
	Conf	0.0128	0.1693	9.9933	11.4195	6.7696	7.3891	4.9003	19.2515	3.7507	4.4411
0.1	Est	0.4166		8.7441		3.5430		2.4837		5.3394	
	Conf	0.3599	0.4733	8.1628	9.3254	3.4282	3.6578	2.2158	2.7517	4.7346	5.9441
50.2	Est	0.1411		11.6363		4.5126		6.8677		4.7302	
Redo	Conf	0.1126	0.1697	11.2239	12.0487	4.4231	4.6021	5.4172	8.3181	4.4054	5.0550

Time differences

Figure 4.15 shows PSA-plots of time differences for the same tests as described in the previous section. The time differences are normalized to the length of the period. For the test on 50.2 Hz, most of the data points are placed in an area where the sum of the differences are close to one period, and most intense in the area closest to differences of 0.5 periods. This means that most of the PDs appear once per half cycle, but at varying places of the half cycle, due to the stochastic element in PDs. If a PD appear early on a half cycle, the difference from the previous PD will probably be smaller than 0.5 periods and the difference to the next will probably be greater than 0.5 periods. There is also an area of PDs with following differences close to 0.25 periods. These data points are a result of two PDs in one half cycle. These data points are few, but seem to be on a line where the sum of the differences are close to 0.5 periods.

The PSA-plot of the time differences from the test at 50.2 Hz, redo, does not have separated areas as the previous plot. An important finding in this plot is that large differences of more than 4 periods, and quite many differences of more than 1 period, meaning that PDs does not appear in each period. It is possible to see an area similar to the most intense area in the previous plot, indicating one PD per half cycle. Additionally there are more intense areas close to the axis with differences at about 0.3-0.6 periods. The differences close to the axis indicate several PDs in the same half cycle. Which is confirmed both by the PSA plot for voltage differences and the PRPD-plot. The cumulative distributions, which are included in Appendix C, also supports these findings.

The PSA-plots for 10 Hz are very similar to the plots for 50.2 Hz. The plots for 5 Hz reveal several periods without discharges, are more like the plot for 50.2 Hz, redo. The plots for the lower frequencies are harder to analyse, but have similarities to the plot for 50.2 Hz, redo.

The PSA plots revealed some trends and supports the previous finding and conclusions. This analysis method is different from the others by analysing sequential PDs, which revealed an absence of PDs in several following periods. Even if there are uncertainties related to this method, have PSA been proven to be a useful tool in the analysis of PDs.

4.10.5 PDIV - PDEV test with grounding conditioning

The tests on Cup with 5 spheres showed a dependency of the history. To investigate the dependency on the initial state, the tests also was performed after 16.5 hours at

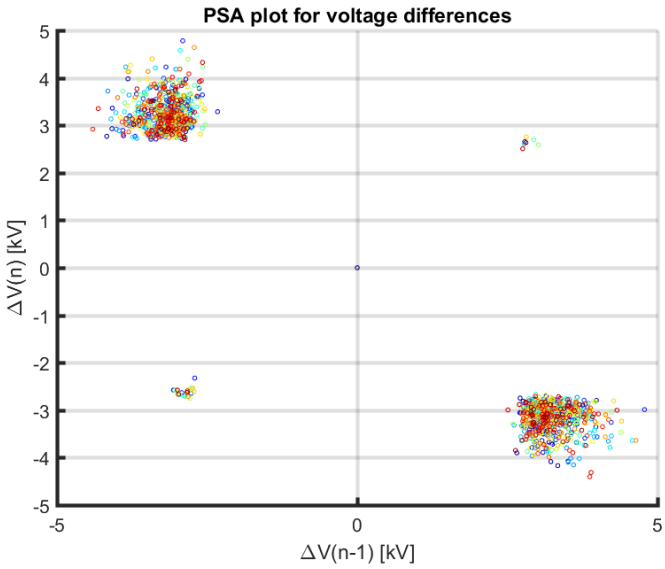

(a) 50.2 Hz

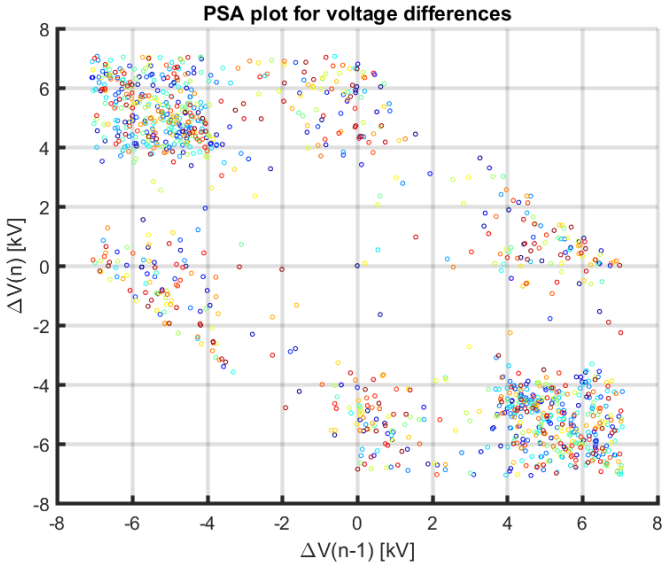

(b) 50.2 Hz, redo

Figure 4.14: These figures show the PSA-plots for the voltage differences. The analysis is performed with the data from the voltage conditioned PDIV-PDEV tests of Cup with 6 spheres at PDIV.

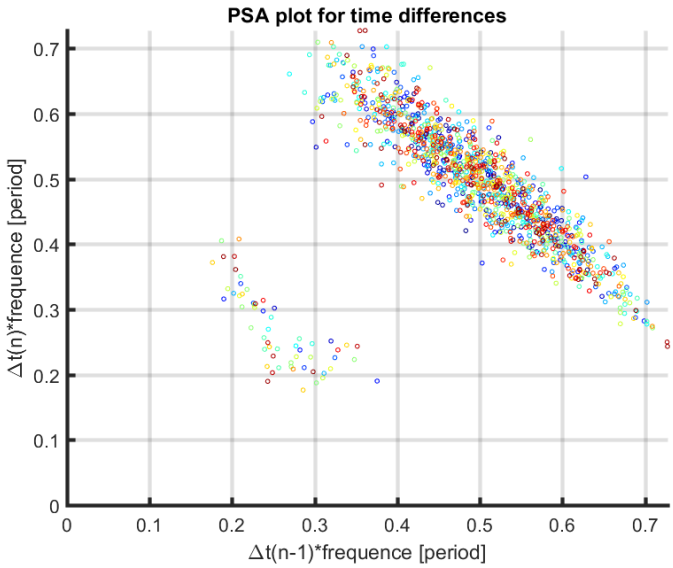

(a) 50.2 Hz

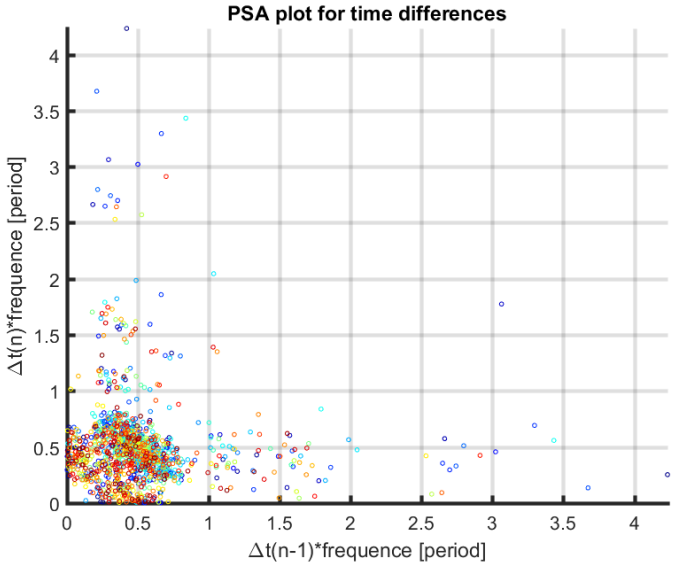

(b) 50.2 Hz, redo

Figure 4.15: These figures show the PSA-plots for the time differences. The analysis is performed with the data from the voltage conditioned PDIV-PDEV tests of Cup with 6 spheres at PDIV.

ground potential. The main focus of this test was to check if there was a difference in the PDIV similar to Cup with 5 spheres. Table 4.9 presents the PDIV, PDEV and other derived parameters found for the different frequencies. The data for 50.2 Hz, Redo are collected at 3.5 kV, due to two discharge sources, the PDIV and PDEV in brackets are for the second PD source. For 50.2, Redo 2 the parameters in brackets are derived from data at PDEV. It was hard to determine both the PDIV and PDEV for the test at 0.1 Hz. PDIV is most likely at 4.0 kV. Due to uncertainty and much noise, the voltage was further risen to 4.5 kV, where the data was collected. PDEV might be be at 3.0 kV or lower, it is hard to determine due to noise.

Figure 4.16 presents sections from the PRPD-plots. The tests at 0.1 Hz and 50.2 Hz, Redo seem to have two PD sources, based on the two visually separable "clouds". At 50.2 Hz, Redo the two clouds had different PDIVs and PDEVs as shown in Table 4.9, which is a good indicator of two separate PD sources. The plots and q_max were very similar for the tests at 10, 5 and 1 Hz. The PDIV varies, which is a result of the stochastic nature of the PDs as earlier explained. The PDEV also varies, this was not expected, but the variations are quite small. In the test at 10 Hz only 50 PDs were recorded the first 15 seconds at 2.0 kV and at 1 Hz with 2.5 kV, there was 4-5 PDs which was in the same area as the earlier PDs. Based on this reasoning, the different PDEVs may only be stochastic variations. The PD source with lowest amplitude at 0.1 Hz and at 50.2 Hz, Redo also give similar PRPD-plots, but these are not analysed further. The PD source at 10, 5, 1 Hz and for the lower "cloud" at 0.1 Hz and 50.2 Hz, Redo is likely to be the same.

The PDs at 50.2 Hz and the PDs with highest amplitude at 0.1 Hz and 50.2 Hz, Redo also have similar PRPD-plots, but q_{max} is much lower at 50.2 Hz compared to the two others. q_{avg} is similar for all the these tests, but in 0.1 Hz and 50.2 Hz, Redo there are two discharge sources, one with higher and one with lower PDs. Therefore, it is possible that the source of the higher PDs in the two last tests are the same, but different from the PD source in the first test. If this is the case, there are three different PD sources in these tests.

The final test at 50.2 Hz, called 50.2 Hz, Redo2, had PRPD-plots different from the earlier in these tests. The plots had no "rabbit-ears" and indicated good availability of start electrons. The PRPD-plots are very similar to the PRPD-plots in the first test with voltage conditioning, as shown in Figure 4.13a. The parameters in brackets in Table 4.9 for 50.2 Hz, Redo2 are derived from data at 2.0 kV, and can be compared to 50.2 Hz in Table 4.6. The repetition rate is equal, but both q_{max} and q_{avg} are higher for the voltage conditioned test. This might be indicating a new PD source. Figure 4.17 shows two following PRPD-plots from the pre-ground conditioning before this last test. These plots show the ignition of a new PD source, confirming a new PD source in the last test with ground conditioning. In total 4 PD

Table 4.9: Derived parameters for ground conditioned tests on Cup with 6 spheres at PDIV. The noise is filtered at 2.5 pC. The data from 50.2, Redo is collected at 3.5 Hz, with two PD sources present. In 50.2, Redo 2 the parameters in brackets are derived from data at 2.0 kV. At 0.1 Hz the parameters are derived from data at 4.5 kV, the others are derived from data at PDIV.

f [Hz]	50.2	10	5	1	0.1	50.2, Redo	50.2, Redo 2
PDIV [kV]	4.0	3.5	3.0	4.5	4.0	4.5 (3.5)	3.5
PDEV [kV]	3.0	2.0	2.5	3.0	3.5	3.0 (2.5)	2.0
n [PDs/period]	1.4	2.4	2.0	3.4	5.3	4.2	4.3 (2.0)
q_{max} [pC]	11.9	8.4	7.8	10.3	23.6	20.5	7.7 (7.5)
q_{avg} [pC]	8.2	4.3	4.4	4.6	8.1	8.3	5.0 (4.9)

sources are observed in this test and in the pre-ground conditioning.

The ignition of a new PD source in the last conditioning period came after more than a month of testing this test object. This proves that the statistical waiting time for virgin cavities can be very long. The late ignition of this PD source is most likely caused by a previously absence of a start electron. Another reason can be electronegative properties of the gas this cavity, but it is more likely a lack of start electrons. Despite a long test duration of this test object, only 4/6 of the spheres where ignited. This indicate either a long statistical waiting time for a start electron or a possibility of not being able to initiate PDs in some spheres. A relatively high conductivity of the inner surface of the spheres, will shield the void interior from the electric field, this can be one of many possible explanations [6].

The tests on Cup with 6 spheres lasted for more than a month, during these tests the start electron availability in the spheres changed. Cup with 5 spheres which also had cavity discharges and gave no indication of such a change. But this test object was only tested for a few days, and might have shown a change with longer testing duration. For Cup with 6 spheres, the change in start electron availability indicate a change in the properties of the spheres, this is not desirable. If the spheres are to be further used, they need to give consistent and reproducible results. The start electron availability will therefore need to reach a steady state, before the parameters used for further testing can be found. To test if the spheres will reach a steady state, a long duration stress test need to be performed, periods of grounding can also be included to test how this affect the start electron availability.

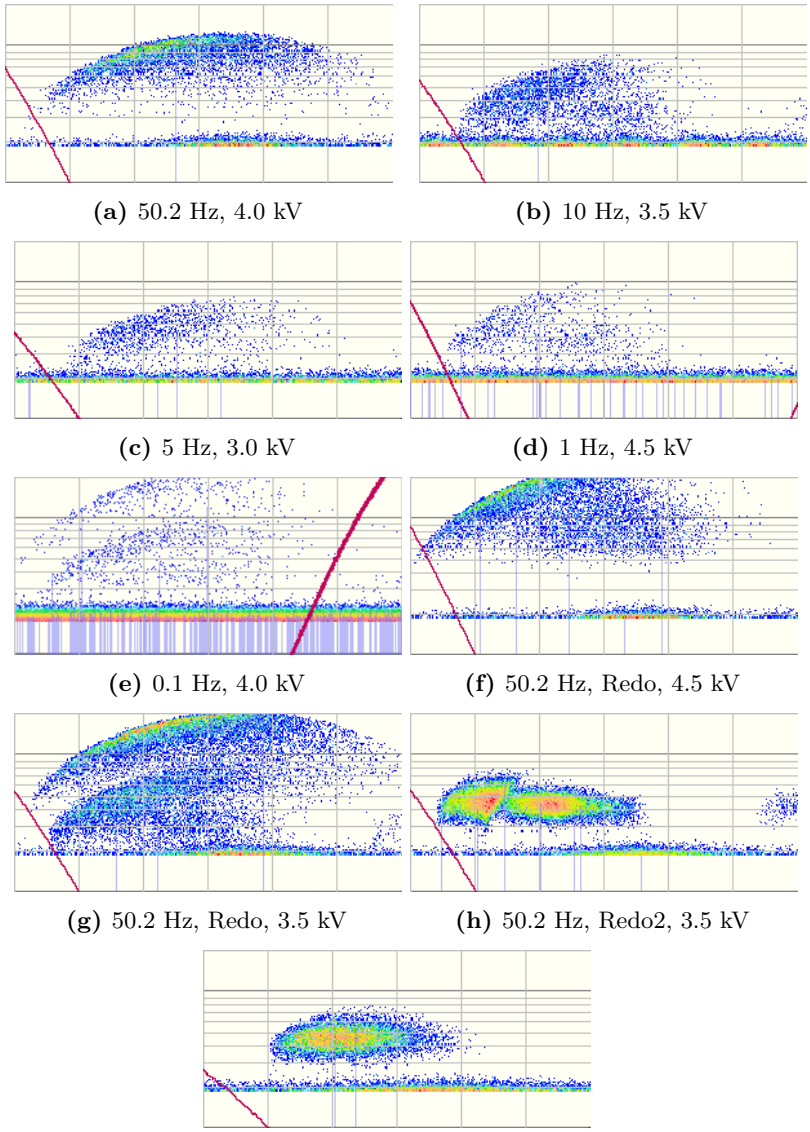

(a) 50.2 Hz, 4.0 kV

(b) 10 Hz, 3.5 kV

(c) 5 Hz, 3.0 kV

(d) 1 Hz, 4.5 kV

(e) 0.1 Hz, 4.0 kV

(f) 50.2 Hz, Redo, 4.5 kV

(g) 50.2 Hz, Redo, 3.5 kV

(h) 50.2 Hz, Redo2, 3.5 kV

(i) 50.2 Hz, Redo2, 2.0 kV

Figure 4.16: These figures show extracted sections of the PRPD-plots from the ground potential conditioned PDIV-tests on Cup with 6 spheres. The sections show the plot between 144° and 360° in a linear scale, 1 pC and 20 pC in a logarithmic scale. At 0.1 Hz the plot is taken from the negative PDs then rotated and flipped due to a large phase shift. The symmetry between the positive and the negative PDs in the PRPD-plot is good.

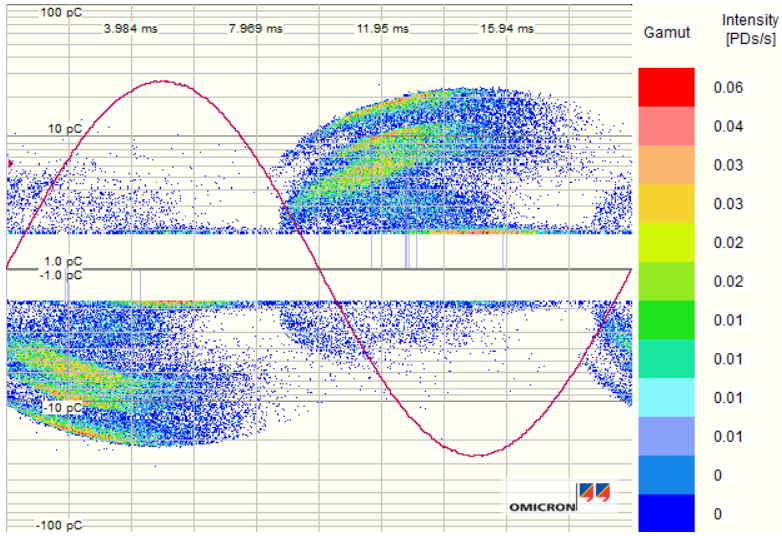

(a) Before ignition

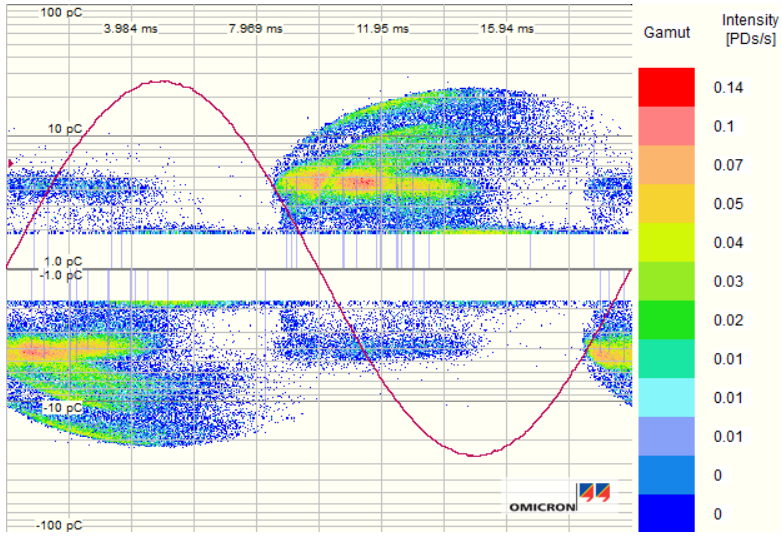

(b) After ignition

Figure 4.17: These figures show two following PRPD-plots from the pre-conditioning before the last PDIV-PDEV test with grounding conditioning of Cup with 6 spheres, called 50.2 Hz, Redo2, at 50.2 Hz and 4.0 kV. The last plot show the ignition of a new discharge source with good start electron availability compared to the other discharge sources.

5 | Conclusion

To determine the local field in a termination or joint with field grading layers, a reproducible PD source could be used, such as a hollow sphere. If hollow glass microspheres are to be included in cable terminations, they need to give reproducible results, no sign of ageing and easy recognisable patterns. The following points are the main findings in this work:

- The procedure with embedding glass hollow microspheres in Rogowski test objects with no electrode paint was found to be successful.
- PDIV was found to be dependent on the initial condition. Thus, a well-defined electrical conditioning of the test object need to be performed to have equal initial condition for each test.
- PDEV was generally consistent and found to be a suitable parameter for further testing.
- From the simulations, the reduction in the repetition rate and Paschen curve, $E_{critical}$ was found to be 1.74 kV/mm in peak value and the pressure inside the cavity equal to 18 kPa.
- Tests were dependent on the availability of start electrons, with good availability of start electrons the *abc*-model explains the results in a good way. In case of poor availability, the Laplacian and the Poisonnian field explain results, with a linear relationship between the applied voltage and the discharge amplitudes.
- The availability of start electrons was in most cases good straight after ignition, but after weeks of testing the availability decreased with time and/or stress. The test objects might need a long conditioning period to reach a steady state period, which give reproducible and consistent results.
- The PRPDA was found to be a very useful tool both in real time analysis and further analysis afterwards. Especially the PRPD-plots with intensity made it

possible to separate different discharge sources and show more intense areas in the patterns indicating repeating PDs from one source.

- The data analysed fitted to Weibull distribution, generally had a good fit with parameters within the range for cavity discharges found in the literature.
- Pulse sequence analysis revealed that some of the tests had several periods with no discharges and also indicated cavity discharges.

Based on the findings in this work, the spheres can be suited for further testing, under the condition of reaching a steady state for the start electron availability.

5.1 Further work

- The tests on Cup with 6 spheres indicated a decrease in the start electron availability during the tests. To test if the start electron availability is further decreased and if it reaches a steady state, the spheres should be tested in a long duration stress test in the range of several weeks. The test can also include periods of grounding, to check if this affects the start electron availability.
- A better procedure for removing the spheres should be developed. A possible solution is to cut a small piece of silicone, containing the sphere, and use a liquid which dissolves silicone, but not glass.
- The spheres need to be tested individually to find the discharge characteristics for each sphere and to be checked if the characteristics are consistent with the findings in this work. A sphere should be molded in new test objects several times to check if the discharges are affected by the orientation of the spheres.
- If new spheres need to be be tested, the PDs can be initiated by weak radiation to reduce the statistic waiting time. This procedure will most likely not affect the measurements after the radiation has been stopped.
- If the start electron availability reaches a steady state and the discharge characteristics are not affected by orientation of the spheres, the spheres can be further tested in cable terminations. For these tests, a sphere needs to be molded into the cable insulation at different distances from the termination of the outer semiconductor. A field grading material needs to be applied to the cable insulation. The PDIV and PDEV is found for different frequencies after a period of electric conditioning. The data from these tests needs to be collected, analysed and compared to the results in this work.
- After the sphere is tested in the cable insulation, the sphere can be grinded to reveal the inner surface of the sphere. The inner surface can be scanned with a topography scanner, and further imported to COMSOL to make an accurate simulation of the field inside the sphere.
- If the spheres used in this work do not give reproducible results, other spheres can be tested at PD sources. Spheres with a smooth inner surface, close to spherical shape, constant wall thickness, known permittivity and resistance from ageing would be preferable to use.

References

[1] E. Lemke, "A critical review of partial-discharge models," *Electrical Insulation Magazine, IEEE*, vol. 28, pp. 11–16, Nov 2012.

[2] "Ieee guide for field testing of shielded power cable systems using very low frequency (vlf)(less than 1 hz)," *IEEE Std 400.2-2013*, pp. 1–60, June 2013.

[3] IEC, *60270, High-voltage test techniques - Partial discharge measurements*, 2000.

[4] C. Forssen and H. Edin, "Partial discharges in a cavity at variable applied frequency part 1: measurements," *Dielectrics and Electrical Insulation, IEEE Transactions on*, vol. 15, no. 6, pp. 1601–1609, 2008.

[5] H. A. Illias, "Measurement and simulation of partial discharges within a spherical cavity in a solid dielectric material." May 2011.

[6] L. Niemeyer, "A generalized approach to partial discharge modeling," *IEEE Transactions on Dielectrics and Electrical Insulation*, vol. 2, pp. 510–528, Aug 1995.

[7] E. Ildstad, *High Voltage Insulation Materials*. NTNU - Department of Electric Power Engineering, 2012.

[8] Cigré, *Guide for Partial Discharges Measuring in Compliance to IEC 60270*, 2008.

[9] J. H. Mason, "Discharge detection and measurements," *Electrical Engineers, Proceedings of the Institution of*, vol. 112, no. 7, pp. 1407–1423, 1965.

[10] C. S. Kim, T. Kondo, and T. Mizutani, "Change in pd pattern with aging," *Dielectrics and Electrical Insulation, IEEE Transactions on*, vol. 11, no. 1, pp. 13–18, 2004.

[11] F. Gutfleisch and L. Niemeyer, "Measurement and simulation of pd in epoxy voids," *Dielectrics and Electrical Insulation, IEEE Transactions on*, vol. 2, no. 5, pp. 729–743, 1995.

[12] L. Lundgaard, "Partielle utladninger begreper, måleteknikk og mulige anvendelser for tilstandskontroll," tech. rep., SINTEF Energi AS, 1996.

[13] C. Cachin and H. J. Wiesmann, "Pd recognition with knowledge-based preprocessing and neural networks," *Dielectrics and Electrical Insulation, IEEE Transactions on*, vol. 2, no. 4, pp. 578–589, 1995.

[14] K. Wu, Y. Suzuoki, T. Mizutani, and H. Xie, "A novel physical model for partial discharge in narrow channels," *Dielectrics and Electrical Insulation, IEEE Transactions on*, vol. 6, pp. 181–190, Apr 1999.

[15] M. Ghaffarian Niasar, H. Edin, X. Wang, and R. C. Kiiza, "Partial discharge characteristics due to air and water vapor bubbles in oil," 2011. QC 2012.

[16] X. Chen, A. Cavallini, and G. C. Montanari, "Improving high voltage transformer reliability through recognition of pd in paper/oil systems," in *High Voltage Engineering and Application, 2008. ICHVE 2008. International Conference on*, pp. 544–548, Nov 2008.

[17] M. Niasar and H. Edin, "Corona in oil as a function of geometry, temperature and humidity," in *Electrical Insulation and Dielectric Phenomena (CEIDP), 2010 Annual Report Conference on*, pp. 1–4, Oct 2010.

[18] C. Heitz, "A generalized model for partial discharge processes based on a stochastic process approach," *Journal of Physics D: Applied Physics*, vol. 32, no. 9, p. 1012, 1999.

[19] Cigré, *KNOWLEDGE RULES FOR PARTIAL DISCHARGE DIAGNOSIS IN SERVICE*, 2003.

[20] A. Contin, G. C. Montanari, and C. Ferraro, "Pd source recognition by weibull processing of pulse height distributions," *IEEE Transactions on Dielectrics and Electrical Insulation*, vol. 7, pp. 48–58, Feb 2000.

[21] M. Cacciari, A. Contin, and G. C. Montanari, "Use of a mixed-weibull distribution for the identification of pd phenomena [corrected version]," *IEEE Transactions on Dielectrics and Electrical Insulation*, vol. 2, pp. 1166–1179, Dec 1995.

[22] E. Eberg, S. Hvidsten, and K. Bergset, "Assessment of overheating in xlpe mv cable joints by partial discharge measurements," *9th International Conference on Insulated Power Cables*, vol. 2, pp. 510–528, Aug 2015.

[23] N. G. Trinh, "Electrode design for testing in uniform field gaps," *Power Apparatus and Systems, IEEE Transactions on*, vol. PAS-99, no. 3, pp. 1235–1242, 1980.

[24] A. Küchler, *Hochspannungstechnik*. Springer-Verlag, 2009.

[25] Wacker Chemie AG, *LIQUID SILICONE RUBBER*, 5 2012. Version: 1.13.

[26] Y. Jing, I. V. Timoshkin, M. P. Wilson, M. J. Given, S. J. Macgregor, T. Wang, and J. M. Lehr, "Dielectric properties of natural ester, synthetic ester midel 7131 and mineral oil diala d," *IEEE Transactions on Dielectrics and Electrical Insulation*, vol. 21, pp. 644–652, April 2014.

[27] OMICRON electronics GmbH, *MPD 600 User Manual*, 2012.

[28] F. Mauseth, H. L. Halvorson, and S. Hvidsten, "Diagnostic testing of thermally aged medium voltage xlpe cable joints," in *Electrical Insulation and Dielectric Phenomena (CEIDP), 2012 Annual Report Conference on*, pp. 823–826, Oct 2012.

[29] G. Einan, "Condition assessment of medium voltage cable accessories," 2015.

[30] M. Ghaffarian Niasar, "Partial discharge signatures of defects in insulation systems consisting of oil and oil-impregnated paper," 2012. QC 20121129.

A | Weibull analysis for voltage conditioning

A.1 50.2 Hz

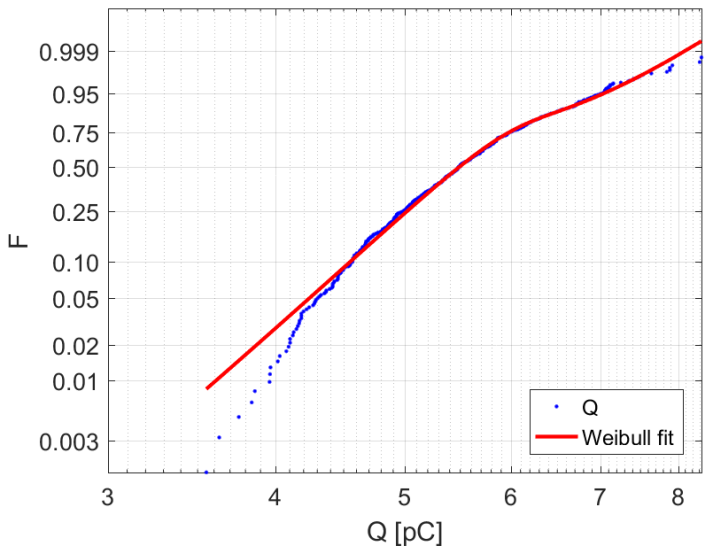

Figure A.1: This figure show the cumulative distribution of positive discharges and the fitted 5-parameter Weibull distribution. The data is collected from the voltage conditioned PDIV-PDEV test on Cup with 6 spheres at PDIV and 50.2 Hz.

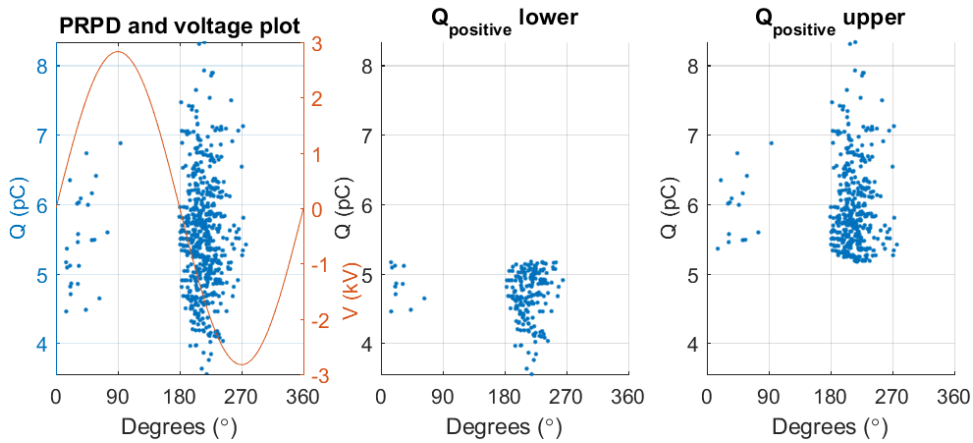

Figure A.2: These figures show PRPD-plots of the positive discharges. The first figure show all the positive discharges plotted with one cycle of the applied voltage. The last two figures show PRPD-plots for each sub-population from the 5-parameter Weibull distribution. The data is collected from the voltage condtioned PDIV-PDEV test on Cup with 6 spheres at PDIV and 50.2 Hz.

A.2 10 Hz

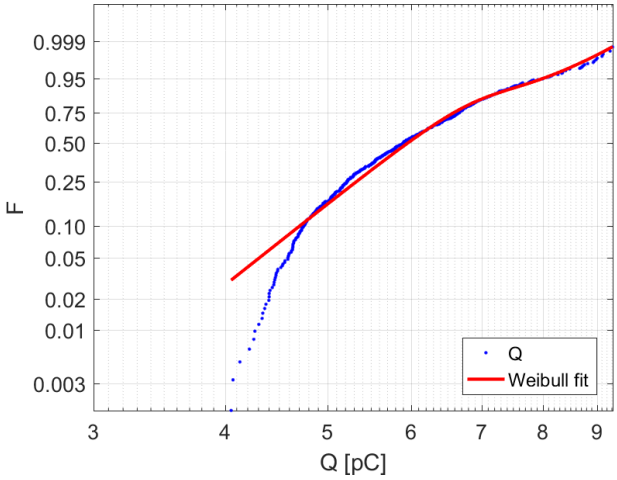

Figure A.3: This figure show the cumulative distribution of positive discharges and the fitted 5-parameter Weibull distribution. The data is collected from the voltage conditioned PDIV-PDEV test on Cup with 6 spheres at PDIV and 10 Hz.

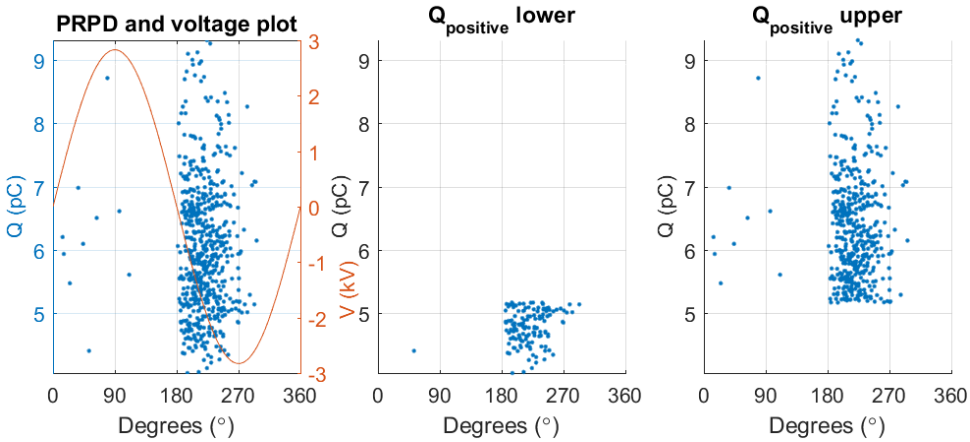

Figure A.4: These figures show PRPD-plots of the positive discharges. The first figure show all the positive discharges plotted with one cycle of the applied voltage. The last two figures show PRPD-plots for each sub-population from the 5-parameter Weibull distribution. The data is collected from the voltage condtioned PDIV-PDEV test on Cup with 6 spheres at PDIV and 10 Hz.

A.3 5 Hz

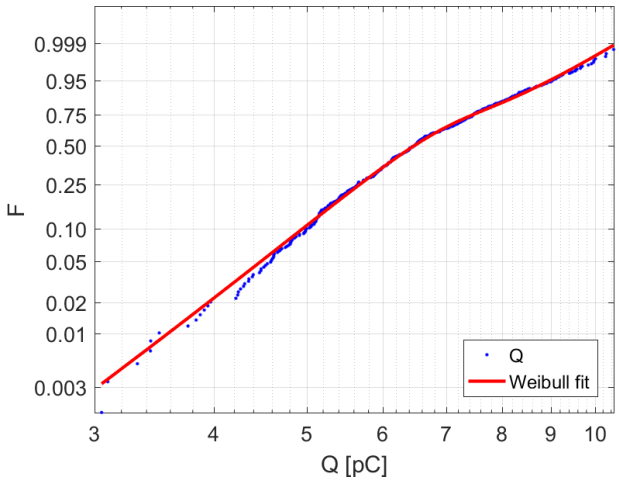

Figure A.5: This figure show the cumulative distribution of positive discharges and the fitted 5-parameter Weibull distribution. The data is collected from the voltage conditioned PDIV-PDEV test on Cup with 6 spheres at PDIV and 5 Hz.

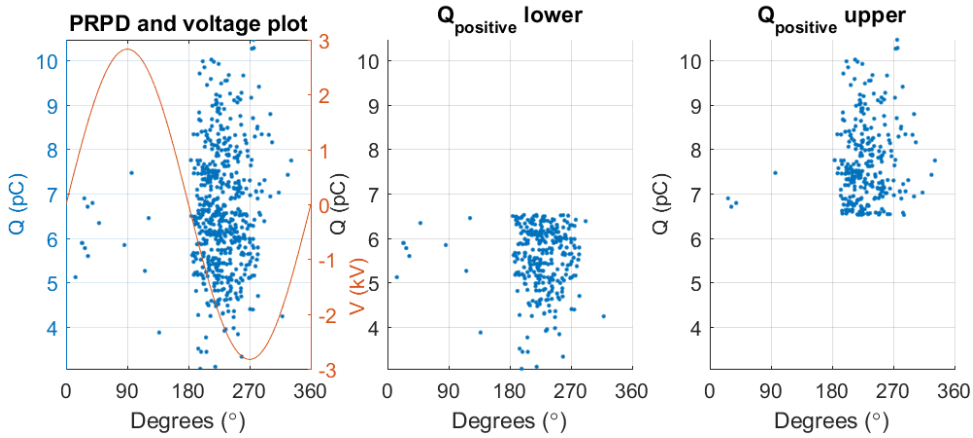

Figure A.6: These figures show PRPD-plots of the positive discharges. The first figure show all the positive discharges plotted with one cycle of the applied voltage. The last two figures show PRPD-plots for each sub-population from the 5-parameter Weibull distribution. The data is collected from the voltage condtioned PDIV-PDEV test on Cup with 6 spheres at PDIV and 5 Hz.

A.4 1 Hz

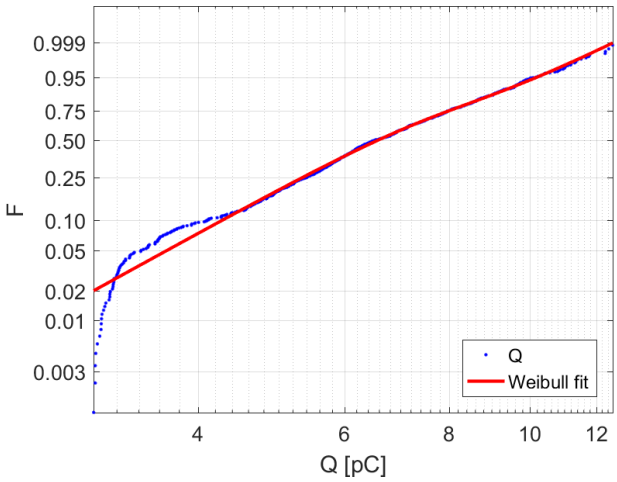

Figure A.7: This figure show the cumulative distribution of positive discharges and the fitted 5-parameter Weibull distribution. The data is collected from the voltage conditioned PDIV-PDEV test on Cup with 6 spheres at PDIV and 1 Hz.

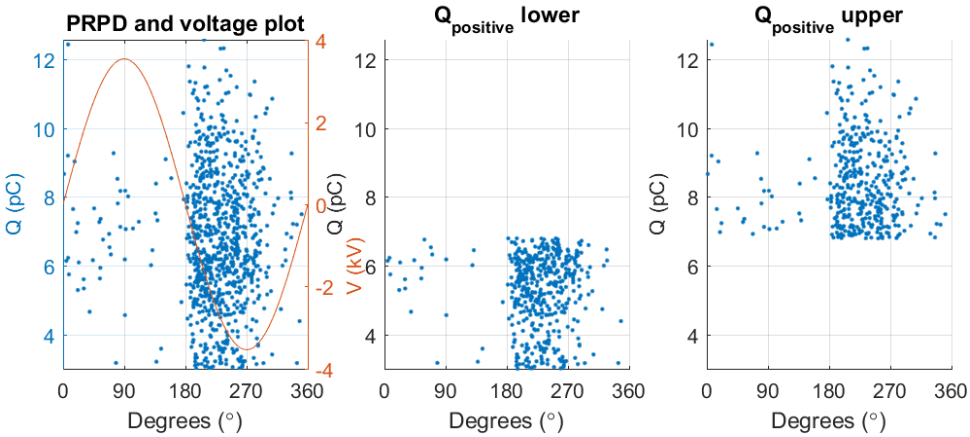

Figure A.8: These figures show PRPD-plots of the positive discharges. The first figure show all the positive discharges plotted with one cycle of the applied voltage. The last two figures show PRPD-plots for each sub-population from the 5-parameter Weibull distribution. The data is collected from the voltage condtioned PDIV-PDEV test on Cup with 6 spheres at PDIV and 1 Hz.

A.5 0.1 Hz

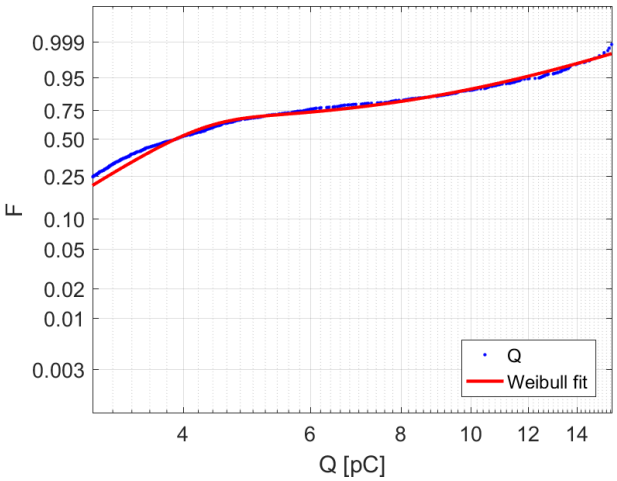

Figure A.9: This figure show the cumulative distribution of positive discharges and the fitted 5-parameter Weibull distribution. The data is collected from the voltage conditioned PDIV-PDEV test on Cup with 6 spheres at PDIV and 0.1 Hz.

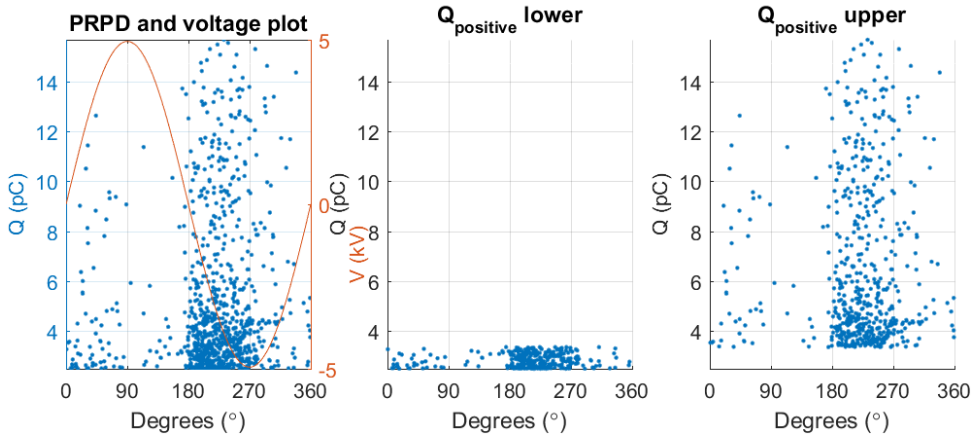

Figure A.10: These figures show PRPD-plots of the positive discharges. The first figure show all the positive discharges plotted with one cycle of the applied voltage. The last two figures show PRPD-plots for each sub-population from the 5-parameter Weibull distribution. The data is collected from the voltage condtioned PDIV-PDEV test on Cup with 6 spheres at PDIV and 0.1 Hz.

A.6 50.2 Hz, redo

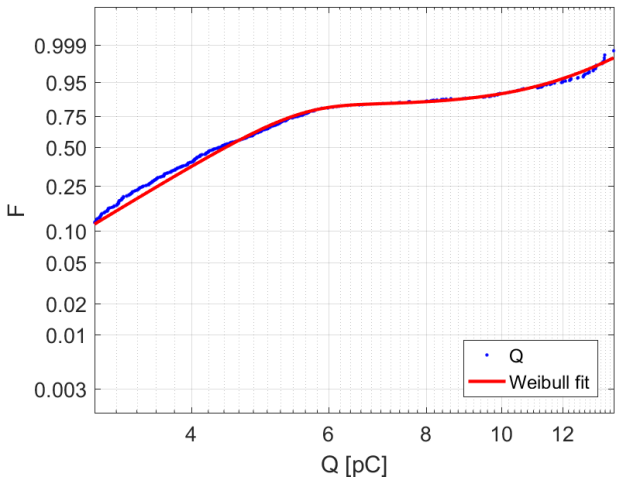

Figure A.11: This figure show the cumulative distribution of positive discharges and the fitted 5-parameter Weibull distribution. The data is collected from the voltage conditioned PDIV-PDEV test on Cup with 6 spheres at PDIV and 50.2 Hz, redo.

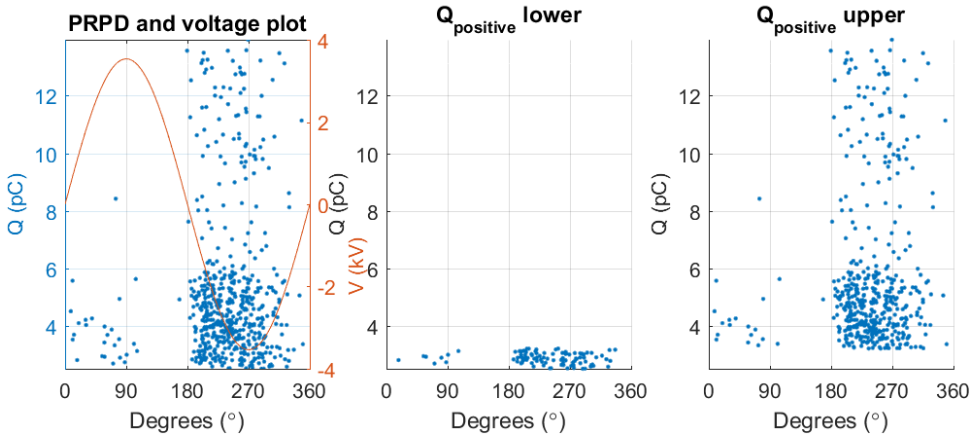

Figure A.12: These figures show PRPD-plots of the positive discharges. The first figure show all the positive discharges plotted with one cycle of the applied voltage. The last two figures show PRPD-plots for each sub-population from the 5-parameter Weibull distribution. The data is collected from the voltage condtioned PDIV-PDEV test on Cup with 6 spheres at PDIV and 50.2 Hz, redo.

B | Periodic varying PD amplitude

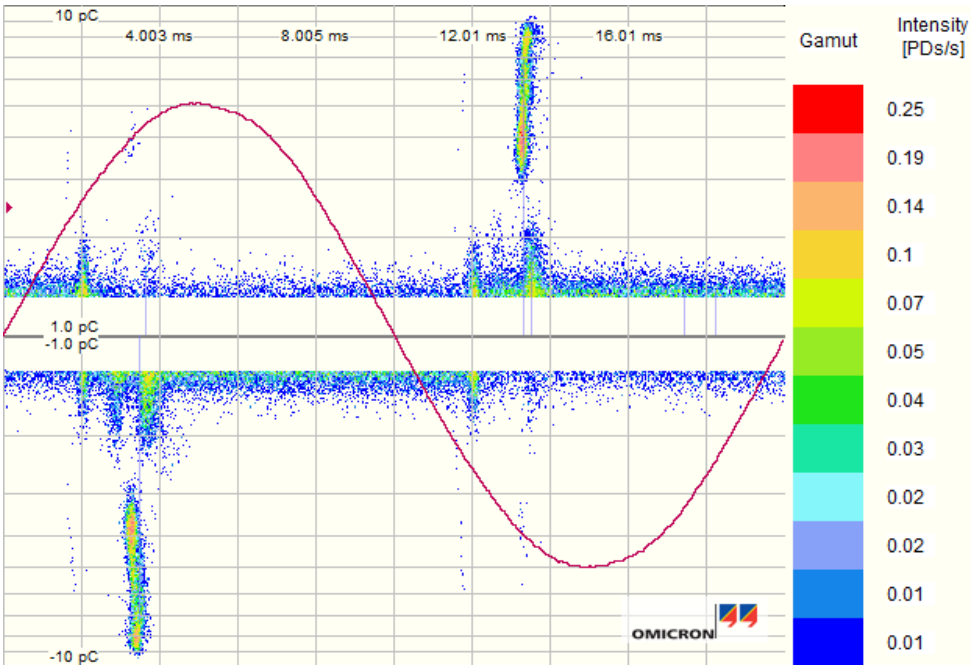

Figure B.1: This figure show the PRPD-plot for the situation of periodic varying PD amplitude found in the test on Cup with sphere No.2. This plot is taken from a test with the transformer at 4.0 kV.

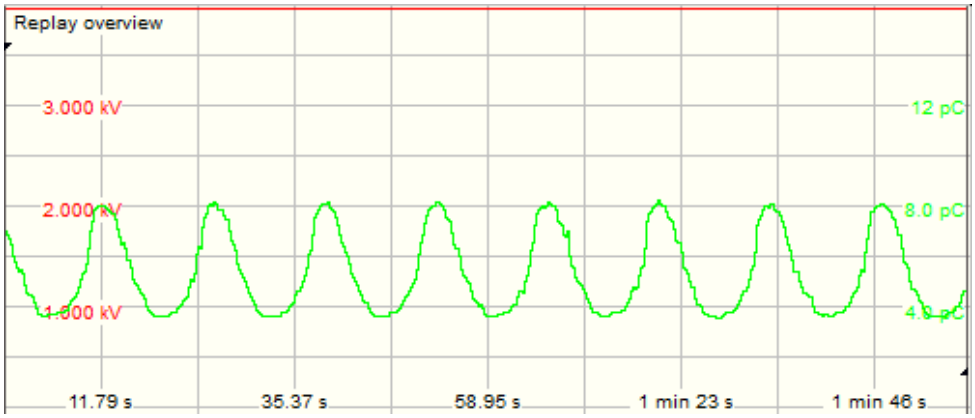

Figure B.2: This figure show the time dependency of the discharge amplitude for the situation of periodic varying PD amplitude found in the test on Cup with sphere No.2. This plot is taken from a test with the transformer at 4.0 kV.

C | PSA

C.1 Cumulative voltage differences

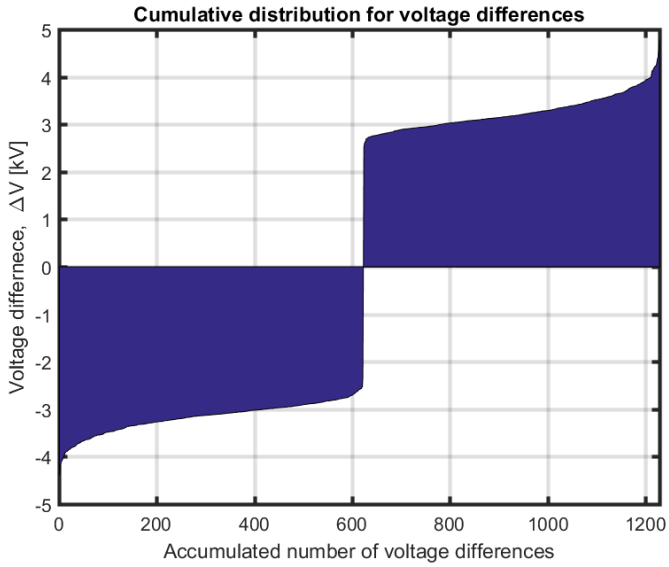

Figure C.1: These figures show the cumulative distribution for the voltage differences. The analysis is performed with the data from the voltage conditioned tests PDIV-PDEV tests of Cup with 6 at PDIV and 50.2 Hz.

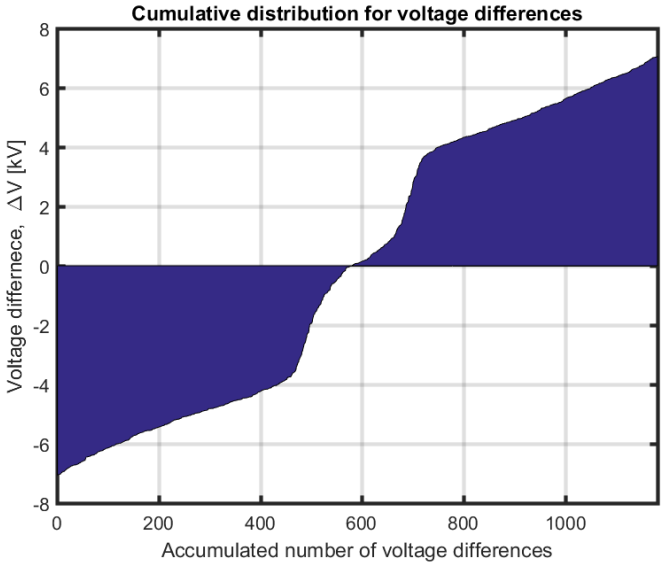

Figure C.2: These figures show the cumulative distribution for the voltage differences. The analysis is performed with the data from the voltage conditioned tests PDIV-PDEV tests of Cup with 6 at PDIV and 50.2 Hz, redo.

C.2 Cumulative time differences

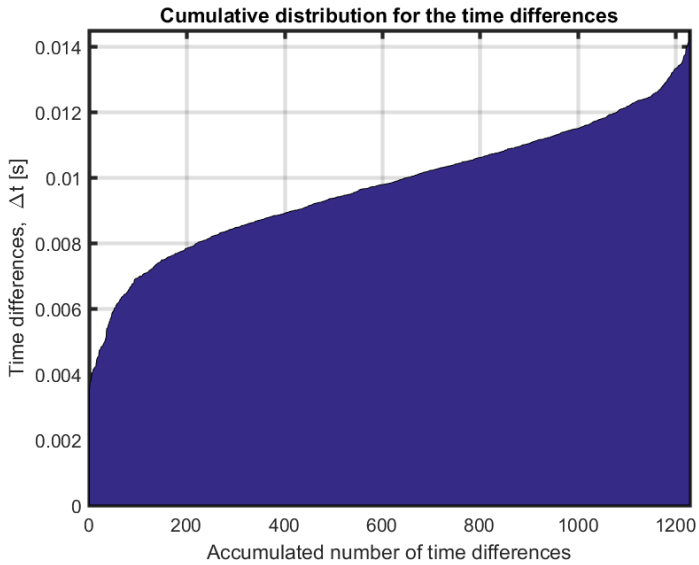

Figure C.3: These figures show the cumulative distribution for the time differences. The analysis is performed with the data from the voltage conditioned tests PDIV-PDEV tests of Cup with 6 at PDIV and 50.2 Hz.

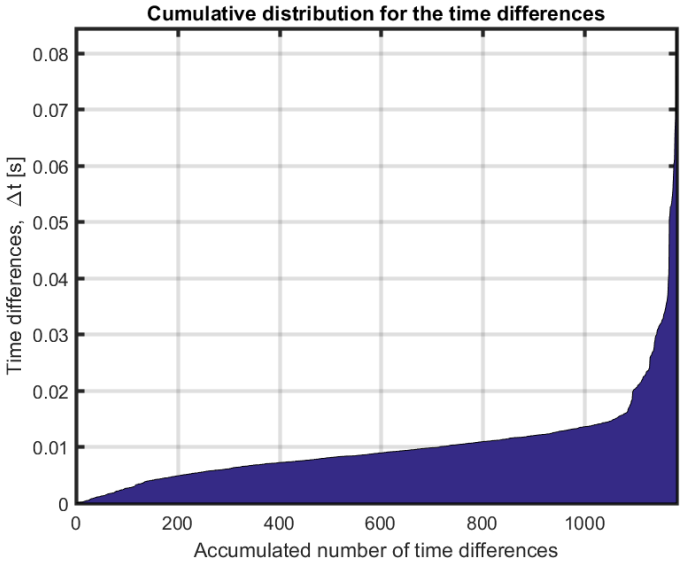

Figure C.4: These figures show the cumulative distribution for the time differences. The analysis is performed with the data from the voltage conditioned tests PDIV-PDEV tests of Cup with 6 at PDIV and 50.2 Hz, redo

D | Matlab-scripts

D.1 Importation

```
ph=importPHdata(path,'unit2.1');
[q_tm, q] = importQdata(path, 'unit2.1');
```

D.2 Phase shift

```
function [ ph_out ] = phase_shift( ph, shift )
%PHASE_SHIFT Summary of this function goes here
%   Detailed explanation goes here
ph_out=ph+shift/360;
ph_out(ph_out<0)=ph_out(ph_out<0)+1;
ph_out(ph_out>1)=ph_out(ph_out>1)-1;
end
```

D.3 Selection of a random sequence of 600 cycles

```
f=50.2;
load('q_ph50_2_G.mat')


l=length(q_tm);

r=ceil(rand(1)*l);
while q_tm(r)>(max(q_tm)-600/f)
    % To ensure a starting point far enough from the (...)
    %end of the matrix. 0.6 because 50Hz is 500 (...)
    % times as large as 0.1Hz, 300sec/500=0.6sec
    r=ceil(rand(1)*l);
```

```
end
i=r;
while (q_tm(i)-q_tm(r))<600/f && i<l
    %To find the correct number of datapoints
    i=i+1;
end
ph=ph(r:i);
q=q(r:i);
q_tm=q_tm(r:i);

save('rand_q_ph50_2_G.mat','ph', 'q', 'q_tm')
```

D.4 Statistical analysis

D.4.1 Positive PDs

```
function [ param_estim, param_conf ] = stat_anal_pos( q )
%STAT_ANAL_50_2_POS Summary of this function goes here
%   Detailed explanation goes here

Qpos = sort(q(q>0))*1e12;

%Define mixed weibull function
pdf_mixedwbl = @(q_var,p,a1,a2,b1,b2) ...
    p*wblpdf(q_var,a1,b1)+(1-p)*wblpdf(q_var,a2,b2);

%Initial conditions
p_start = .5;
start_param = wblfit(Qpos);
start = [p_start start_param(1) start_param(1)...
    start_param(2) start_param(2)];

%Boundaries
lb = [0 0 0 0 0];
ub = [1 5000 5000 100 100];

options = statset('MaxIter',1000, 'MaxFunEvals',2000);

[param_estim, param_conf] = mle(Qpos, 'pdf',...
    pdf_mixedwbl, 'start', start, ...
     'lower', lb, 'upper', ub, 'Options', options)

npos = length(Qpos)+1;
probpos = (1:npos-.3)./(npos+0.4);
ypos = log(log(1./(1-probpos)));

F = param_estim(1)*wblcdf(Qpos,param_estim(2),...
    param_estim(4))+(1-param_estim(1))*wblcdf...
```

```
33      (Qpos,param_estim(3),param_estim(5));
34
35  F_min = param_conf(2,1)*wblcdf(Qpos,param_conf...
36      (1,2),param_conf(1,4))+ (1-param_conf(2,1))...
37      *wblcdf(Qpos,param_conf(1,3),param_conf(2,5));
38
39  F_max = param_conf(1,1)*wblcdf(Qpos,param_conf...
40      (2,2),param_conf(2,4))+ (1-param_conf(1,1))...
41      *wblcdf(Qpos,param_conf(2,3),param_conf(1,5));
42
43  figure(31), ...
44      semilogx((Qpos),(ypos),'b.')
45      hold on
46      semilogx((Qpos),log(log(1./(1-F))),'r', ...
47          'linewidth', 2)
48
49
50      p = [0.001 0.003 0.01 0.02 0.05 ...
51          0.10 0.25 0.5 0.75 0.95 0.999];
52      label = {'0.001','0.003', '0.01','0.02',...
53          '0.05','0.10','0.25','0.50','0.75','0.95',...
54          '0.999'};
55
56      tick  = log(log(1./(1-p)));
57      set(gca, 'YTick', tick);
58      set(gca, 'YTickLabel', label,'fontsize',13);
59      grid on
60
61      ylim([log(log(1./(1-0))) log(log(1./(1-.9999999)))])
62      xlim([3 max(Qpos)])
63
64
65      xlabel('Q [pC]')
66      ylabel('F')
67      legend('Q','Weibull fit','location','SouthEast')
68
69  hold off
70
71  print Weibull_pos -dpng
72  end
```

D.4.2 Negative PDs

```
1  function [ param_estim, param_conf ] = stat_anal_neg( q )
2  %STAT_ANAL_50_2_NEG Summary of this function goes here
3  %   Detailed explanation goes here
4
5  Qneg = sort(abs(q(q<0)))*1e12;
6
7  %Define mixed weibull function
```

```
pdf_mixedwbl = @(q_var,p,a1,a2,b1,b2) ...
    p*wblpdf(q_var,a1,b1)+(1-p)*wblpdf(q_var,a2,b2);

%Initial conditions
p_start = .5;
start_param = wblfit(Qneg);
start = [p_start start_param(1) start_param(1) ...
    start_param(2) start_param(2)];

%Boundaries
lb = [0 0 0 0 0];
ub = [1 5000 5000 100 100];

options = statset('MaxIter',1000, 'MaxFunEvals',2000);

[param_estim, param_conf] = mle(Qneg, 'pdf',...
    pdf_mixedwbl, 'start', start,...
    'lower', lb, 'upper', ub, 'Options', options)

nneg = length(Qneg)+1;
probneg = (1:nneg-.3)./(nneg+0.4);
yneg = log(log(1./(1-probneg)));

F = param_estim(1)*wblcdf(Qneg,param_estim(2)...
    ,param_estim(4))+ (1-param_estim(1))...
    *wblcdf(Qneg,param_estim(3),param_estim(5));

F2_min = param_conf(2,1)*wblcdf(Qneg,param_conf(1,2)...
    ,param_conf(1,4))+ 1-param_conf(2,1))...
    *wblcdf(Qneg,param_conf(1,3),param_conf(2,5));

F2_max = param_conf(1,1)*wblcdf(Qneg,param_conf(2,2)...
    ,param_conf(2,4))+(1-param_conf(1,1))...
    *wblcdf(Qneg,param_conf(2,3),param_conf(1,5));


    p= [0.001 0.003 0.01 0.02 0.05 0.10...
        0.25 0.5 0.75 0.95 0.999];
    label   = {'0.001','0.003', '0.01','0.02','0.05'...
        ,'0.10','0.25','0.50','0.75','0.95', '0.999'};

 figure(32), ...
    semilogx((Qneg),(yneg),'b.')
    hold on
    semilogx((Qneg),log(log(1./(1-F))),'r',...
        'linewidth', 2)

    tick  = log(log(1./(1-p)));
    set(gca, 'YTick', tick);
    set(gca, 'YTickLabel', label,'fontsize',13);
    grid on

```

```
60      ylim([log(log(1./(1-0))) log(log(1./(1-.9999999)))])
61      xlim([3 max(Qneg)])
62
63
64      xlabel('Q [pC]')
65      ylabel('F')
66   %   title('50.2 Hz, redo - 2.5 kV - Q_{neg}' ,'fontsize',13)
67      legend('Q','Weibull fit','location','SouthEast')
68
69  hold off
70
71  print Weibull_neg -dpng
72
73  end
```

D.5 Weibull separated PRPDA

```
1   function [  ] = PRPD( ph,q, p_pos, p_neg,v_rms )
2   %PRPD Summary of this function goes here
3   %   Detailed explanation goes here
4   q=q*1e12;
5   ph=ph*360;
6   q_pos=sort(q(q>0));
7   ph_pos=ph(q>0);
8   q_neg=sort(abs(q(q<0)));
9   ph_neg=ph(q<0);
10
11  t=0:0.1:360;
12  v=sqrt(2)*v_rms*sin(2*pi*t/360);
13
14  figure(11)
15  set(gcf,'units','centimeters','position',[5,5,20,7]);
16  %set(gca,'TightInset')
17  subplot(1,3,1)
18  grid on
19  yyaxis left
20  scatter(ph_pos,q_pos,'.')
21  yyaxis right
22  plot(t,v);
23  title('PRPD and voltage plot')
24  xlabel('Degrees (\circ)')
25  xlim([0, 360])
26  set(gca, 'XTick' ,[0 90 180 270 360]);
27  yyaxis left
28  ylabel('Q (pC)','fontsize',10)
29  ylim([min(q_pos) max(q_pos)])
30  yyaxis right
31  y2=ylabel('V (kV)','fontsize',10);
32  set(y2,'position',get(y2,'position')-[0 1.5 0])
```

```
33
34 subplot(1,3,2)
35 scatter(ph_pos(1:round(p_pos*length(q_pos))),...
36     q_pos(1:round(p_pos*length(q_pos))),'.');
37 grid on
38 xlabel('Degrees (\circ)')
39 ylabel('Q (pC)','fontsize',10)
40 xlim([0, 360])
41 set(gca, 'XTick' ,[0 90 180 270 360]);
42 ylim([min(q_pos) max(q_pos)])
43 title('Q_{positive} lower')
44
45 subplot(1,3,3)
46 scatter(ph_pos(round(p_pos*length(q_pos)):length(q_pos)),...
47     q_pos(round(p_pos*length(q_pos)):length(q_pos)),'.');
48 grid on
49 xlabel('Degrees (\circ)')
50 ylabel('Q (pC)','fontsize',10)
51 xlim([0, 360])
52 set(gca, 'XTick' ,[0 90 180 270 360]);
53 ylim([min(q_pos) max(q_pos)])
54 title('Q_{positive} upper')
55
56 tightfig;
57
58 print PRPD_weibull_pos -dpng
59
60 %%%%%%%%%%%%%%%%%%%%%%%%%%%%%%%%%%%%%%%%%%%%%%%%%%%%%%%%%%%%%%%%%%%%%%%%
61
62 figure(12)
63 set(gcf,'units','centimeters','position',[7,7,20,7]);
64
65 subplot(1,3,1)
66 grid on
67 yyaxis left
68 scatter(ph_neg,q_neg,'.')
69 yyaxis right
70 plot(t,v);
71 title('PRPD and voltage plot')
72 xlabel('Degrees (\circ)')
73 xlim([0, 360])
74 set(gca, 'XTick' ,[0 90 180 270 360]);
75 yyaxis left
76 ylabel('Q (pC)','fontsize',10);
77 %get(y1,'position')
78 ylim([min(q_neg) max(q_neg)])
79 yyaxis right
80 y1=ylabel('V (kV)','fontsize',10);
81 set(y1,'position',get(y1,'position')-[0 1.5 0])
82
83 subplot(1,3,2)
84 scatter(ph_neg(1:round(p_neg*length(q_neg))),...
```

```
    q_neg(1:round(p_neg*length(q_neg))),'.');
grid on
xlabel('Degrees (\circ)')
ylabel('Q (pC)','fontsize',10)
xlim([0, 360])
set(gca, 'XTick' ,[0 90 180 270 360]);
ylim([min(q_neg) max(q_neg)])
title('Q_{negative} lower')

subplot(1,3,3)
scatter(ph_neg(round(p_neg*length(q_neg)):length(q_neg)),...
    q_neg(round(p_neg*length(q_neg)):length(q_neg)),'.');
grid on
xlabel('Degrees (\circ)')
ylabel('Q (pC)','fontsize',10)
xlim([0, 360])
set(gca, 'XTick' ,[0 90 180 270 360]);
ylim([min(q_neg) max(q_neg)])
title('Q_{negative} upper')

tightfig;

print PRPD_weibull_neg -dpng

end
```

D.6 PSA

```
function [ ] = PSA( ph,q_tm, v_rms, freq )
%PSA Summary of this function goes here
%   Detailed explanation goes here

%v=sqrt(2)*v_rms*sin(2*pi*ph);


%tidsintervall
n = length(q_tm); %q_tm er tidspunkt for kvar enkelt PD
t_n1 = zeros(n-2,1);
t_n2 = zeros(n-2,1);

for i = 2:n-1
    t_n1(i-1) = q_tm(i)-q_tm(i-1);
    %tidsforskjell mellom aktuell PD og forrige
    t_n2(i-1) = q_tm(i+1)-q_tm(i);
    %tidsforskjell mellom aktuall PD og neste
end

delta_t = t_n1;
delta_t(n-1) = t_n2(n-2); %t_n1 mangler differansen mellom dei to siste PD
```

```
22 delta_t = sort(delta_t);
23
24 figure(21);
25 area(delta_t);
26 title('Cumulative distribution for the time differences');
27 xlim([0, length(delta_t)])
28 ylim([0, max(delta_t)])
29 xlabel('Accumulated number of time differences')
30 ylabel('Time differences,  \Deltat [s]')
31 set(gca, 'YGrid' , 'on' ,'XGrid','on','LineWidth' ,2 , 'fontsize',10)
32 print Cumulative_time -dpng
33
34 %Spenningsdifferanse
35 V_n1 = zeros(n-2,1);
36 V_n2 = zeros(n-2,1);
37 m = length(ph);
38 for i = 2:m-1
39   V_n1(i) = sqrt(2)*v_rms*sin(2*pi*ph(i))-sqrt(2)*v_rms*sin(2*pi*ph(i-1));
40   %Spenningsdifferanse mellom aktuell PD og forrige
41   V_n2(i) = sqrt(2)*v_rms*sin(2*pi*ph(i+1))-sqrt(2)*v_rms*sin(2*pi*ph(i));
42   %Spenningsdifferanse mellom aktuell PD og neste
43 end
44
45 figure(22);
46 plot(V_n1,V_n2,'xr');
47 title('PSA plot for voltage differences')
48 xlabel('\DeltaV(n-1) [-]')
49 ylabel('\DeltaV(n) [-]')
50
51 %Sorterte spenningsdifferanser
52 delta_V = V_n1;
53 delta_V(n-1) = V_n2(n-2); %V_n1 mangler differansen mellom dei to siste PD
54 delta_V = sort(delta_V);
55
56 figure(23);
57 area(delta_V);
58 title('Cumulative distribution for voltage differences');
59 xlim([0, length(delta_V)])
60 xlabel('Accumulated number of voltage differences')
61 ylabel('Voltage differnece,  \DeltaV [-]')
62 set(gca, 'YGrid' , 'on' ,'XGrid','on','LineWidth' ,2 , 'fontsize',10)
63 print Cumultaive_voltage -dpng
64
65 cmp=jet(n-2);
66 figure(24);
67 scatter(t_n1*freq,t_n2*freq,5,cmp);
68
69 title('PSA plot for time differences')
70 xlabel('\Deltat(n-1)*frequence [period]')
71 ylabel('\Deltat(n)*frequence [period]')
72 set(gca, 'YGrid' , 'on' ,'XGrid','on','LineWidth' ,2 , 'fontsize',10)
73 xlim([0,max(t_n1*freq)])
```

```
ylim([0,max(t_n2*freq)])
print PSA_time -dpng

%Spenningsintervall med histogram
cmp=jet(n-1);
figure(25);
scatter(V_n1,V_n2,5,cmp);
title('PSA plot for voltage differences')
xlabel('\DeltaV(n-1) [-]')
ylabel('\DeltaV(n) [-]')
set(gca, 'YGrid' , 'on' ,'XGrid','on','LineWidth' ,2 , 'fontsize',10)
print PSA_voltage -dpng

end
```

D.7 Main script

```
disp('Velkommen!')
load('rand_q_ph50_2_G');
freq=50.2;%input('Skriv inn frekvens: ');
V=4;%input('Skriv inn spenning i kV: ');
ph_shift=0;%input('Skriv inn faseskifte i grader: ');

if ph_shift ==0
else
    ph=phase_shift(ph,ph_shift);
end

[param_pos,conf_pos]=stat_anal_pos(q);
[param_neg,conf_neg]=stat_anal_neg(q);

PRPD(ph,q,param_pos(1),param_neg(1),V);

PSA(ph,q_tm,V,freq);

save('weibull_param.mat', 'param_pos' , 'param_neg',...
    'conf_pos', 'conf_neg')
```